Cell

Host Remodeling of the Gut Microbiome and Metabolic Changes during Pregnancy

Omry Koren,[1] Julia K. Goodrich,[1] Tyler C. Cullender,[1] Aymé Spor,[1,11] Kirsi Laitinen,[3,4] Helene Kling Bäckhed,[6,7] Antonio Gonzalez,[8] Jeffrey J. Werner,[2,12] Largus T. Angenent,[2] Rob Knight,[9,10] Fredrik Bäckhed,[6,7] Erika Isolauri,[5] Seppo Salminen,[4] and Ruth E. Ley[1,*]

[1]Department of Microbiology and Department of Molecular Biology and Genetics
[2]Department of Biological and Environmental Engineering
Cornell University, Ithaca, NY 14853, USA
[3]Institute of Biomedicine
[4]Functional Foods Forum
University of Turku, 20610 Turku, Finland
[5]Department of Pediatrics, Turku University Hospital, 20521 Turku, Finland
[6]Sahlgrenska Center for Cardiovascular and Metabolic Research/Wallenberg Laboratory, SE-413 45 Gothenburg, Sweden
[7]Department of Molecular and Clinical Medicine, University of Gothenburg, SE-405 30 Gothenburg, Sweden
[8]Department of Computer Science
[9]Department of Chemistry and Biochemistry
[10]Howard Hughes Medical Institute
University of Colorado, Boulder, Boulder, CO 80309, USA
[11]Present address: INRA, UMR1347 Agroécologie, 21000 Dijon, France
[12]Present address: Department of Chemistry, SUNY Cortland, Cortland, NY 13045, USA
*Correspondence: rel222@cornell.edu
http://dx.doi.org/10.1016/j.cell.2012.07.008

SUMMARY

Many of the immune and metabolic changes occurring during normal pregnancy also describe metabolic syndrome. Gut microbiota can cause symptoms of metabolic syndrome in nonpregnant hosts. Here, to explore their role in pregnancy, we characterized fecal bacteria of 91 pregnant women of varying prepregnancy BMIs and gestational diabetes status and their infants. Similarities between infant-mother microbiotas increased with children's age, and the infant microbiota was unaffected by mother's health status. Gut microbiota changed dramatically from first (T1) to third (T3) trimesters, with vast expansion of diversity between mothers, an overall increase in Proteobacteria and Actinobacteria, and reduced richness. T3 stool showed strongest signs of inflammation and energy loss; however, microbiome gene repertoires were constant between trimesters. When transferred to germ-free mice, T3 microbiota induced greater adiposity and insulin insensitivity compared to T1. Our findings indicate that host-microbial interactions that impact host metabolism can occur and may be beneficial in pregnancy.

INTRODUCTION

Over the course of a normal, healthy pregnancy, the body undergoes substantial hormonal, immunological, and metabolic changes (Mor and Cardenas, 2010; Newbern and Freemark, 2011). Body fat increases early in pregnancy, followed by reduced insulin sensitivity later in gestation (Barbour et al., 2007). Reduced insulin sensitivity has been correlated with changes in immune status in pregnancy, including elevated levels of circulating cytokines (e.g., TNF-α and IL-6; Kirwan et al., 2002) that are thought to drive obesity-associated metabolic inflammation (Gregor and Hotamisligil, 2011). In contrast to the obese state where they are detrimental to long-term health, excess adiposity and loss of insulin sensitivity are beneficial in the context of a normal pregnancy, as they support growth of the fetus and prepare the body for the energetic demands of lactation (Di Cianni et al., 2003; Lain and Catalano, 2007; Nelson et al., 2010).

The cause of reduced insulin sensitivity in pregnancy remains unclear. In the context of nonpregnant obesity, recent work suggests a role for gut microbiota in driving metabolic disease, including inflammation, weight gain, and reduced insulin sensitivity (Cani et al., 2007; Vijay-Kumar et al., 2010). The gut microbiota is shaped by environmental factors, such as diet (Wu et al., 2011), host genetics (Spor et al., 2011), and the immune system, which, in particular, can have profound effects on the composition of the gut microbiota (Salzman et al., 2010; Slack et al., 2009; Vijay-Kumar et al., 2010). In pregnancy, immunological changes occur at the placental interface to inhibit rejection of the fetus, while at the mother's mucosal surfaces, elevated inflammatory responses often result in exacerbated bacterially mediated diseases, such as vaginosis and gingivitis (Beigi et al., 2007; Straka, 2011). In the gut, bacterial load is reported to increase over the course of gestation (Collado et al., 2008), but a comprehensive view of how microbial diversity changes over the course

of normal pregnancy is lacking. The contribution of intestinal host-microbial interactions in promoting weight gain and other metabolic changes in the context of pregnancy remains to be evaluated.

In the present study, we have characterized the changes in the gut microbiota that occur from the first (T1) to the third (T3) trimester of pregnancy and have assessed the potential of T1 and T3 microbiota to induce metabolic changes using germ-free (GF) mouse transfers. We provide evidence that the gut microbial community composition and structure are profoundly altered over the course of pregnancy. Furthermore, the T3 microbiota induces metabolic changes in GF recipient mice that are similar to aspects of metabolic syndrome. These changes are associated with metabolic disease in nonpregnant women and men but may be beneficial in the context of a normal pregnancy.

RESULTS

The Gut Microbiota Is Profoundly Altered during Pregnancy

To address how pregnancy alters the gut microbiome, we obtained stool samples, diet information, and clinical data for 91 pregnant women who were previously recruited for a prospective, randomized mother-infant nutrition study in Finland (see Supplemental Information available online for details; Collado et al., 2008, 2010; Laitinen et al., 2009). Each pregnant woman donated stool during T1 (13.84 ± 0.16 weeks) and T3 (33.72 ± 0.12 weeks) of pregnancy, and a subset donated stool 1 month postpartum. Additionally, a stool sample was obtained from the women's infants at 1 month of age, and a subset was resampled at 6 months and 4 years of age. Prior to pregnancy, the majority of the women in the study had normal body weights, although a subset was either overweight or obese (Table S1), and 15 women were diagnosed with gestational diabetes mellitus (GDM; Table S1). The women's diets at T1 and T3 were evaluated by nutritionists by using 3 day food records; 16 of the women took probiotic supplements over the course of pregnancy, and 7 used antibiotics at either T1 or T2 (see Supplemental Information; Laitinen et al., 2009). Health markers (i.e., HOMA, GHbA1C1, insulin, and four others) and anthropometric measurement indicators of adiposity gains were obtained during clinical visits (Table 1). Overall, the diets of the women, including total energy intake, were unchanged between sampling times. From T1 to T3, the women gained adiposity and had higher integrated levels of circulating glucose (i.e., higher GHbA1c1), greater circulating levels of leptin, insulin, and cholesterol, and increased insulin resistance (i.e., significant changes in HOMA and QUICKI values; Table 1).

We employed a culture-independent approach to compare the gut microbial communities of women during pregnancy (T1 and T3) and postpartum and of their children at the different ages. PCR was used to amplify the V1V2 variable region of the 16S ribosomal RNA (rRNA) gene, and samples were multiplexed and pyrosequenced, followed by quality filtering and chimera checking (see Experimental Procedures), which yielded 925,048 high-quality 16S rRNA gene sequences (average per sample: 2,873 ± 156). We then clustered sequences into operational taxonomic units (OTUs; clustered at 97% pairwise sequence identity) and assigned taxonomies. We applied the UniFrac distance metric (Lozupone and Knight, 2005), which provides a measure of the evolutionary distance between microbiotas (β-diversity), to assess pregnancy effects on between-individual variation in community composition. The weighted UniFrac analysis (sensitive to abundances of taxa) revealed a dramatic expansion of β-diversity with gestational age (Figure 1A), and the unweighted UniFrac analysis (sensitive to rarer taxa) showed a global shift in microbial community composition from T1 to T3 (Figure S1A). The magnitude of the change in β-diversity (weighted and unweighted UniFrac) from T1 to T3 was unrelated to prepregnancy body mass index (BMI), GDM development, or previous number of births (Figures 1B–1D, S1B, and S1C). Within individual women, we could not relate changes in β-diversity to their health status before or during pregnancy nor to their use of probiotics or antibiotics during pregnancy (Table 1; Supplemental Information for additional analyses). Additionally, although we used the same techniques that have previously shown relationships between OTU abundances and components of the diet (Wu et al., 2011), we did not detect any significant relationships between aspects of the microbiota and our diet records either within or between trimesters (see Supplemental Information for details), which may reflect other methodological differences between these two studies. The lack of any correlations between covariates studied here and changes in β-diversity between trimesters raises the possibility that they may be related to immune or hormonal changes.

From T1 to T3, the relative abundances of Proteobacteria increased on average (T1, 0.73% ± 0.08%; T3, 3.2% ± 0.68%; $p = 0.0004$), as did Actinobacteria (T1, 5.1% ± 0.47%; T3, 9.3% ± 1.32%; $p = 0.003$; paired t tests; Figure 2A; see Data S1 for full taxonomic information by sample), and although these changes did not occur in all subjects, they occurred in 69.5% and 57% of women, respectively. Figure 1 indicates that the greatest component of the variation between samples (PC1, 33%) relates to the gradient of Bacteroidetes and Firmicutes abundances across samples (Figures 1E and 1F) and that the separation of T3 samples from T1 along PC2 reflects enrichment of Proteobacteria in many of the T3 samples (Figure 1G).

The number of OTUs was significantly reduced as individual women progressed from T1 to T3 (T1, 219 ± 4.1; T3, 161 ± 5.8; paired t test $p \leq 0.0001$; note that enterotypes were not present within trimesters; see Supplemental Information). Similarly, T1 microbial communities had greater within-sample (α) phylogenetic diversity than T3 microbiota, regardless of prepregnancy BMI and health state (Figure 1H and Table S2). T1 samples also had significantly more even taxonomic distributions than T3 samples (Gini coefficients; Table S2). Together with β-diversity patterns, these findings indicate that, by T3, microbiotas were depleted of bacterial phylogenetic diversity in ways that differed between individuals.

We used machine learning techniques to identify 29 OTUs whose relative abundance reliably discriminated T1 and T3 samples (clustering confidence >80%; Figure 2B). Eighteen of these discriminatory OTUs were overrepresented in T1 and belonged mostly to the Clostridiales order of the Firmicutes (e.g., butyrate producers, such as *Faecalibacterium* and

Table 1. Diets and Health Characteristics of Pregnant Women in T1 and T3

		T1	T3	p value[a]
Diet	Energy intake (kcal/day)	1961.45 (±44.77)	2060.40 (±54.63)	0.1411
	Fat intake (g/day)	68.73 (±2.08)	71.59 (±2.79)	0.3807
	Carbohydrates intake (g/day)	248.00 (±6.71)	261.76 (±6.95)	0.1217
	Protein intake (g/day)	80.80 (±2.00)	84.99 (±2.16)	0.1523
	Total fiber intake (g/day)	19.84 (±0.75)	21.30 (±0.77)	0.1311
	Soluble fiber intake (g/day)	5.22 (±0.22)	5.59 (±0.26)	0.3306
	Nonsoluble fiber intake (g/day)	7.98 (±0.34)	8.24 (±0.32)	0.5855
	Saturated fatty acids (g/day)	28.42 (±0.93)	28.60 (±1.33)	0.9878
	Monounsaturated fatty acids (g/day)	22.99 (±0.78)	24.15 (±0.98)	0.2965
	Polyunsaturated fatty acids (g/day)	11.16 (±0.50)	12.24 (±0.55)	0.1198
	Starch (g/day)	102.12 (±3.05)	107.13 (±2.92)	0.1615
	Vegetable use (g/day)	288.88 (±13.45)	276.95 (±11.89)	0.4171
	Fruits and berries use (g/day)	339.80 (±26.92)	330.05 (±19.98)	0.4754
	Cereal (g/day)	206.94 (±7.92)	217.45 (±7.94)	0.3762
	Milk products (g/day)	576.23 (±28.84)	640.01 (±30.72)	0.1322
	Sour milk products (g/day)	175.57 (±15.64)	164.59 (±14.91)	0.4218
	Meat (g/day)	98.35 (±5.46)	99.05 (±5.80)	0.8630
	Sucrose (g/day)	44.57 (±2.15)	47.41 (±2.76)	0.3927
Anthropometric measurements	Biceps[b] (cm)	10.28 (±0.56)	10.61 (±0.59)	0.4303
	Triceps[b] (cm)[f]	21.24 (±0.59)	22.15 (±0.63)	0.0125
	Subsca[b] (cm)[f]	16.58 (±0.64)	19.03 (±0.68)	5.14×10^{-10}
	Hip[c] (cm)[f]	103.84 (±0.82)	106.80 (±0.82)	6.95×10^{-16}
	Mid. upper arm muscle[c] (cm)	23.86 (±0.30)	24.37 (±0.40)	0.1054
Plasma measurements	Leptin (ng/ml)[f]	30.72 (±1.83)	37.58 (±2.47)	0.0008
	Cholesterol (mmol/l)[f]	4.76 (±0.09)	6.37 (±0.12)	1.72×10^{-33}
	Insulin (mU/l)[f]	6.48 (±0.59)	10.92 (±0.88)	1.01×10^{-8}
	Homeostatic model assessment (HOMA)[f]	1.35 (±0.12)	2.28 (±0.19)	1.93×10^{-7}
	Quantitative insulin sensitivity check index (QUICKI)[f]	0.39 (±0.01)	0.35 (±0.00)	2.39×10^{-9}
	Glucose (mmol/l)	4.65 (±0.03)	4.61 (±0.05)	0.5799
	GHbA1c1 (%)[f]	5.01 (±0.03)	5.23 (±0.03)	9.92×10^{-10}
Cytokines[d,e]	IL-2 (pg/g)[g]	15.31 (±0.36)	19.80 (±0.74)	
	IL-4 (pg/g)	15.96 (±0.58)	18.42 (±0.79)	
	IL-6 (pg/g)[g]	12.48 (±0.43)	17.85 (±0.93)	
	IL-8 (pg/g)[g]	14.83 (±0.58)	11.79 (±0.57)	
	IL-10 (pg/g)	15.03 (±0.32)	13.56 (±0.48)	
	GM-CSF (pg/g)	32.40 (±1.34)	37.30 (±1.96)	
	IFNγ (pg/g)[g]	61.87(±4.55)	71.33 (±4.00)	
	TNFα (pg/g)[g]	19.52 (±1.23)	24.95 (±1.18)	

[a]FDR was calculated for each category (diet, anthropometric measurements, and plasma measurements) by using the Benjamini Hochberg correction.
[b]Skinfold thickness; subsca, subscapular skinfold thickness.
[c]Circumference.
[d]n = 67 mothers.
[e]Units are pg/g dry stool.
[f]Significantly different between trimesters, two-tailed paired t test, $p < 0.05$ with FDR correction.
[g]ANOVA $p < 0.05$.

Eubacterium; Figure 2B). OTUs that were overrepresented in the T3 samples included members of the Enterobacteriaceae family and *Streptococcus* genus (Figure S2). No correlations were found between the abundances of specific OTUs (at any level of taxonomy) and the use of probiotics, antibiotics, number of previous births, health markers, or the diet data (see

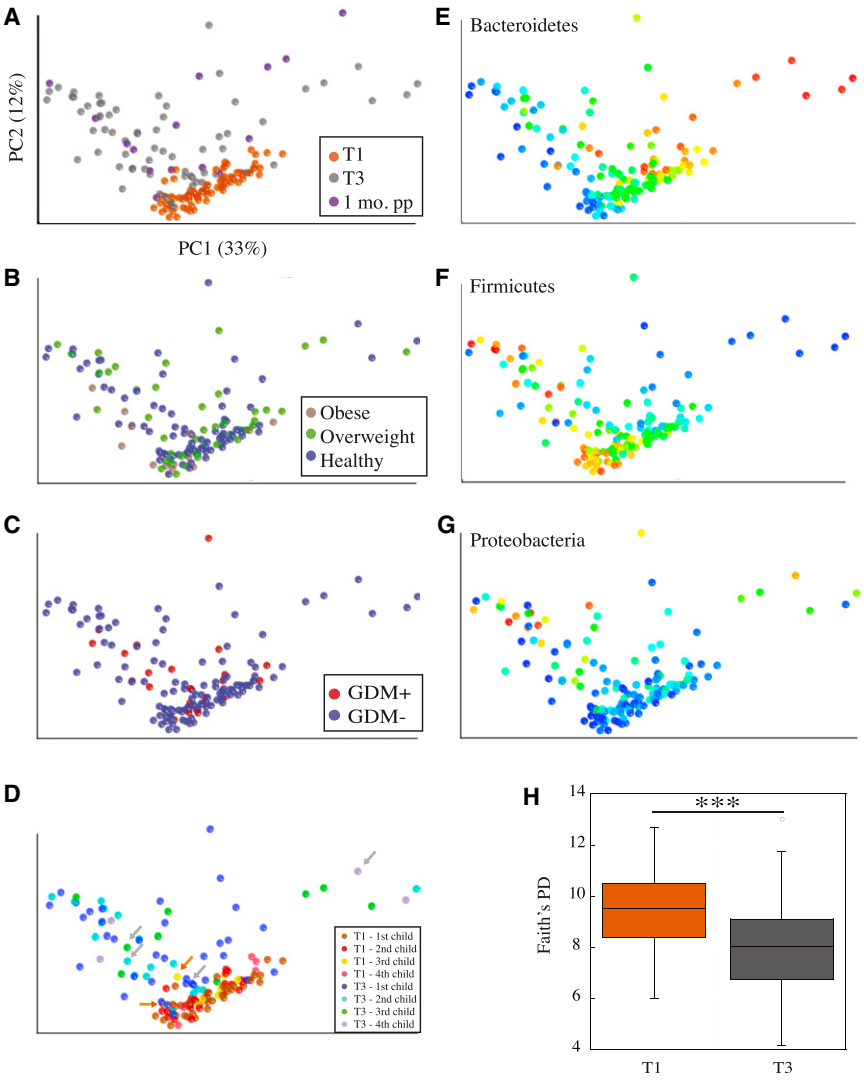

Figure 1. 16S rRNA Gene Surveys Reveal Changes to Microbial Diversity during Pregnancy

(A–G) Microbial communities clustered using PCoA of the weighted UniFrac matrix. The percentage of variation explained by the principal coordinates is indicated on the axes. The same plots are shown for (A)–(G), except 1 month postpartum samples are additionally included in (A). Each point corresponds to a community colored by T1, T3, or 1 month postpartum (A); prepregnancy BMI (B); gestational diabetes (GDM; C); trimester and birth order of expected child (D); abundance gradient of Bacteroidetes (E); abundance gradient of Firmicutes (F); and abundance gradient of Proteobacteria (G). Arrows in (D) point to samples from women who received antibiotics in T1 (orange arrows) and T2 (not T3, gray arrows). (E–G) Gradients are colored from low abundance (blue) to high abundance (red).

(H) Boxplots for community richness (α-diversity) for T1 and T3 samples. For both T1 and T3, data shown are Faith's phylogenetic diversity (PD) for 100 iterations of 790 randomly selected sequences/sample. ***$p < 0.0001$.

See Figure S1.

length reference set (Greengenes; see Experimental Procedures). A combined weighted UniFrac analysis showed clearly that the β-diversity of T1 is similar to HMP normal controls (Figures 3 and S3A). In contrast, the T3 β-diversity is far higher than for T1 and HMP samples (Figure 3). The combined Principal Coordinates Analysis (PCoA) of the UniFrac matrix shows a separation of T1 samples from HMP controls along PC1, reflecting differences in Bacteroidetes and Firmicutes content (Figures 1E and 1F). This indicates that the between-individual variation is similar for T1 and HMP samples, even though the community structure for these samples differs somewhat. Various factors may account for the compositional differences between the sample sets, but the difference between the pregnancy samples and the HMP samples is much larger than the difference between the HMP stool assayed with two different primer regions (Figure S3A), such that primer region is not an explanatory factor for this shift. However, in contrast to the HMP protocol, we lyophilized our samples prior to homogenization and DNA extraction, and our comparison of handling methods on a small subset of samples indicates that handling may also account for part of the shift (Figures S3B and S3C). It is also highly likely that either the onset of pregnancy (i.e., hormonal or behavioral changes) induces a shift in composition reflected in PC1 and/or the provenance of the samples (Finland versus USA) may be important, as geographical/cultural factors have been shown to impact gut microbial diversity (De Filippo et al., 2010; Yatsunenko et al., 2012).

Supplemental Information for details on the statistical tests employed to search for associations; Table 1). These results indicate changes in immunity and/or hormonal levels may also induce changes in phylogenetic content of the microbiota.

T1 Microbial Diversity Is Normal, and T3 Diversity Is Aberrant

The large differences in β-diversity for T1 and T3 samples raised the question of which of these two sets of pregnancy samples was most similar to the nonpregnant state. To answer this question, we placed our data in the context of the Human Microbiome Project's (HMP) recently generated healthy reference data set of microbial diversity across the human body (Human Microbiome Project Consortium, 2012), which includes 16S rRNA gene sequences for 191 stool samples obtained from 98 men and 93 nonpregnant women. The HMP 16S rRNA gene sequence data consisted of two different regions of the 16S rRNA gene (both V1V2 and V3V5); therefore, we compared these sets to our data by picking OTUs against a common full-

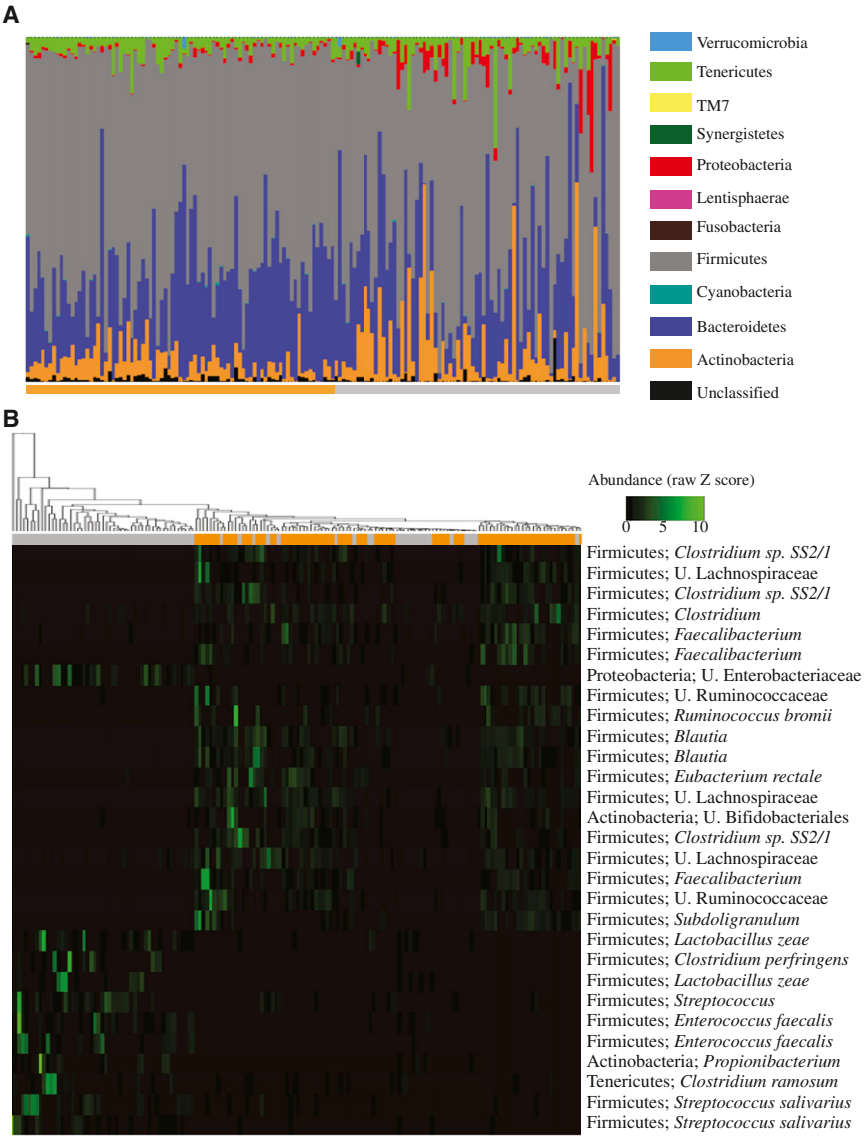

Figure 2. Abundances of Phyla and Enrichment of Bacterial Genera in T1 versus T3

(A) Relative abundances of the phyla present in samples for T1 (left, orange bar) and T3 (right, gray bar). Colors correspond to phyla (see legend).

(B) Heatmap of OTU abundances found to discriminate between T1 and T3 by machine learning. Counts were standardized (Z score, shown in legend) prior to unsupervised hierarchical clustering of samples (columns). The color bar indicates the origin of the samples (T1, orange; T3, gray). The taxonomic assignment of each OTU is indicated to the right of the rows (OTUs; note several OTUs may share the same taxonomic assignment).

See Figure S2.

Shift in Bacterial Diversity Is Unrelated to Health State

We tested whether the change in β-diversity from T1 to T3 was driven by samples obtained from women who had above-normal prepregnancy BMIs or who developed GDM. Results showed that women who were overweight or obese prior to pregnancy and women who developed GDM also had a significant shift in β-diversity from T1 to T3 (weighted and unweighted UniFrac, Figures S3D and S3E). Removal of these subjects from the whole data set showed that the shift from T1 to T3 also occurred in the healthy women alone (Figures S3D and S3E). These results strongly suggest that the expansion of β-diversity between women is a widely shared phenomenon driven by pregnancy, regardless of health status.

We further observed that women who were obese prior to pregnancy had the lowest within-subject (α) diversity at both T1 and T3, although this was not significantly different from normal-weight women. In addition, GDM+ women tended to have the most depleted microbial richness at T1 (Table S2), although their microbiotas did not differ in composition from those of matched controls (Figures 1C and S1C; no significant differences for OTU abundances; false discovery rate [FDR] of 0.05). Importantly, GDM did not negatively impact the microbiotas of the children. Children of GDM+ mothers did not differ from children of GDM− mothers in terms of their microbiotas' α-diversity, Gini coefficients, or OTU abundances (FDR of 0.05). These results suggest that, although a low phylogenetic diversity may be a biomarker for GDM, this condition does not appear to negatively impact the microbiotas of infants born to GDM+ mothers.

High β-Diversity Persists Postpartum and Occurs in Infants

The high levels of between-individual variation in community composition observed in T3 persisted for women 1 month postpartum (Figures 1A and 4). We found that the relative abundance of the genus *Streptococcus*, which is significantly enriched in T3 and 1-month-postpartum samples compared to T1, is in highest abundance in the 1 month olds (analysis of variance [ANOVA] for children's data, $p \leq 0.05$; Figure S2). Additionally, infants age 1 month and 6 months also had elevated levels of β-diversity, but by 4 years of age, children had levels of β-diversity similar to mothers at T1 (Figure 4). These results indicate that differences in gut microbiota between infants are higher than what is observed in nonpregnant adults, as previously reported (Koenig et al., 2011; Palmer et al., 2007). (It is important to note that the V1V2 region primers used in this study are biased against *Bifidobacteria* [Kuczynski et al., 2012], an important component of the developing infant microbiota [Koenig et al., 2011], although this bias has been shown not to impact the diversity of other taxa [Sim et al., 2012].) Using UniFrac to measure microbiota distances between mother-infant

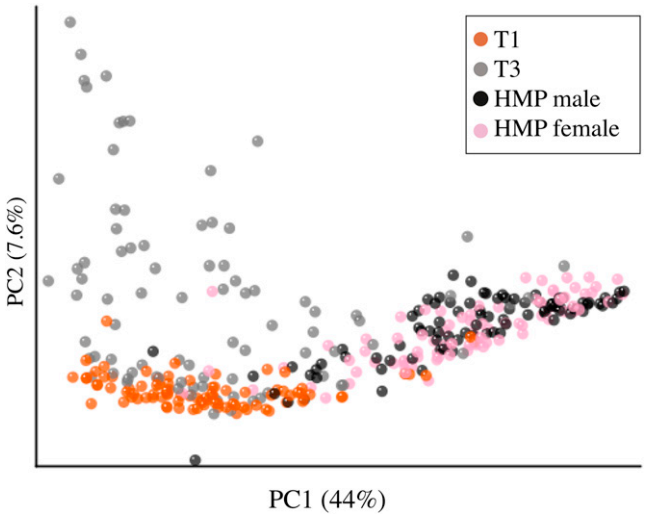

Figure 3. Microbial Diversity of T1 Samples Is More Similar to Nonpregnant HMP Controls Than T3 Samples

PCoA of the weighted UniFrac distances between T1 (orange), T3 (gray), normal healthy HMP male (black), and female (pink) controls. Each symbol represents a sample. The percent of variation explained by the PCs is indicated in parentheses on the axes.

See Figure S3.

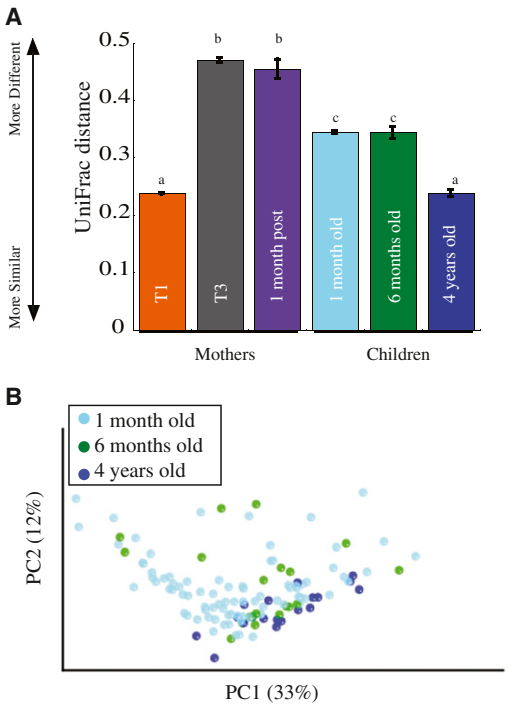

Figure 4. High Between-Individual Microbial Diversity in T3 Persists in the Women Postpartum and Is Observed in Their Neonates

(A) Mean weighted (±SEM) UniFrac distances between bacterial communities of women (sampled at T1, T3, and 1 month postpartum) and their children (1 month, 6 months, and 4 years old). Different letters on bars indicate that means are significantly different at $p \leq 0.05$.

(B) PCoA plot of weighted UniFrac distance matrix, percent variation explained by PCs is indicated on the axes. Each symbol represents a child's microbiota, colored by age.

See Figure S4.

pairs, we found that the T1 microbiota was more similar to the children's microbiota at all ages than the T3 (Figure S4). Although infant/child microbiotas (at all ages) were not more similar to their own mothers' microbiotas compared to unrelated mothers' microbiotas (at T1), the similarity to their own mother was greatest for the 4 year olds (weighted UniFrac p value = 0.003, paired t test). These patterns are consistent with observations that within-family similarities in microbiomes are observed for older children, but not for infants (Turnbaugh et al., 2009a; Yatsunenko et al., 2012).

Stool Energy Content and Metagenomic Analysis

Gut microbial community composition has been linked to how efficiently energy can be extracted from components of the diet reaching the colon and undergoing bacterial fermentation (Jumpertz et al., 2011; Turnbaugh et al., 2006, 2009a, 2009b). Thus, we asked whether changes in community structure could be related to energy loss in stool. Using bomb calorimetry, we measured a significant increase in stool energy content between trimesters within individual women (4.4 ± 0.6 versus 4.7 ± 0.6 Kcal/gram dry weight [gdw]; p = 0.002; paired t test). This difference in stool energy content (i.e., ~10%) has been considered relevant to host adiposity in studies of obese and lean mice (Turnbaugh et al., 2006) and for altered microbiomes associated with excess nutrient load (Jumpertz et al., 2011). Here, however, these changes in stool energy content may not be related to diet or levels of food energy intake because these remained constant from T1 to T3 (Table 1) but may be related to changes in host energy uptake or gut microbiota.

Previous studies have shown that a microbiome's energy extraction efficiency from the diet is correlated with an enrichment of specific metabolic pathways, particularly those for carbohydrate transport and utilization (Turnbaugh et al., 2006, 2009a). To assess whether this was the case for the T1 versus T3 microbiomes, we performed a shotgun metagenomic analysis of T1 and T3 samples obtained from ten mothers selected at random (Figure S5A) by using the Illumina HiSeq 2000 ($4.1 \times 10^7 \pm 5.9 \times 10^6$ sequences/sample; Table S3). The metagenome-based community composition matched the 16S rRNA-based phylogenetic profile (Figure S5B). Unlike patterns observed in obesity-associated microbiomes, this analysis did not reveal differences in the mean relative abundance of gene categories (clusters of orthologous groups, COGs) or metabolic pathways (Kyoto Encyclopedia of Genes and Genomes, KEGG) between trimesters (Figure 5A). This finding may reflect the similar abundances of the major phyla across trimesters. Levels of Bacteroidetes and Firmicutes, which can impact microbiome gene content (Turnbaugh et al., 2006), were not significantly different between trimesters (Figure 5B). It was interesting to note, however, that a network analysis of correlations between COG abundances across samples (using the maximal information-based nonparametric exploration [MINE] statistics; Reshef et al., 2011) indicated that the T1 functional network had a lower degree of random connectivity between functionally unrelated

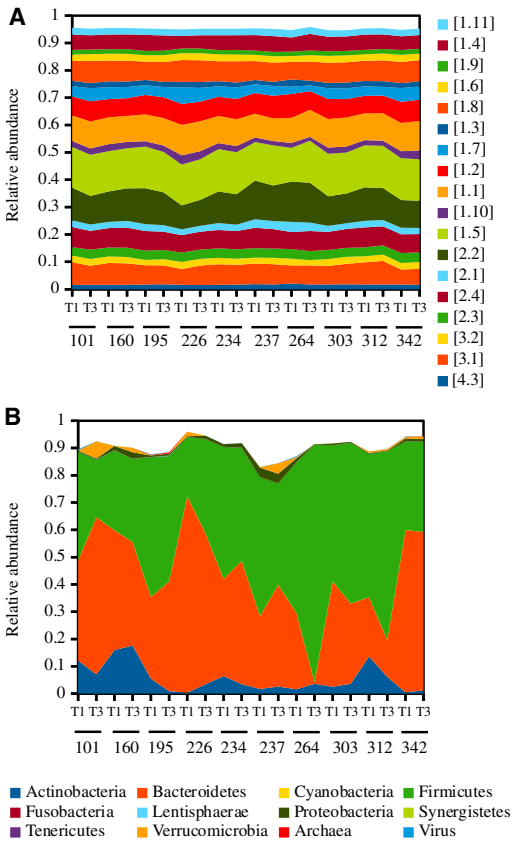

Figure 5. Comparison of Functional Variation and Taxonomic Abundances in T1 and T3 Microbiomes

(A) Relative abundances of gene categories across 20 microbiomes (10 women, each sampled at T1 and T3), based on MG-RAST functional categories (numbers in legend correlate to gene categories in the KEGG pathway database; see Supplemental Information).

(B) Relative taxonomic abundances based on MG-RAST taxonomic classification of shotgun reads. Colors relate to taxa in legend. Numbers at the bottom of the figures refer to mother ID.

See Figure S5.

genes and a greater degree of modularity than the T3 network (modularity of 0.69 versus 0.64; Figures S5C–S5H). Disease-associated microbiomes have recently been shown to consist of less modular metabolic networks compared to health-associated microbiomes (Greenblum et al., 2012). The loss of network modularity in T3 is likely related to reduced phylogenetic diversity and the more uneven distribution of taxa. Overall, the metagenomic analysis indicated that the shifts in microbiome during pregnancy are not associated with the functional changes previously observed in the context of obesity (Ley et al., 2005; Turnbaugh et al., 2006) and may not be linked directly to the energy content of the stool.

Transfer of T3 Microbiota Induces Greater Adiposity and Inflammation in Germ-free Recipient Mice Than T1 Microbiota

The higher average proportion of Proteobacteria in T3 microbiota (Figure 2A), including elevated levels of Enterobacteriaceae, raised the question of whether the T3 microbiota can induce a greater inflammatory response in the host compared to T1 microbiota, as Proteobacteria are often associated with inflammatory conditions (Mukhopadhya et al., 2012). To address this question, we first measured levels of cytokines in T1 and T3 stool (stool cytokine levels can be biomarkers for inflammation in the gut [Saiki et al., 1998]). Levels of the proinflammatory cytokines IFN-γ, IL-2, IL-6, and TNF-α were significantly higher in T3 than in T1 (Tukey's Honestly Significant Difference [HSD] test; $p \leq 0.05$, $p \leq 0.001$, $p \leq 0.001$, and $p \leq 0.005$, respectively; Tables 1 and S4). Although pregnancy is associated with anti-inflammatory conditions at the placental interface (Mor and Cardenas, 2010), our data suggest that the T3 mucosal surfaces of the gastrointestinal tract present low-grade inflammation.

A powerful approach to investigate whether changes in the microbiota are a cause or a consequence of greater levels of inflammation is to transfer microbiotas to GF wild-type recipient mice, which can be colonized with human microbiotas in a manner that maintains the complex communities of the original donor samples (Turnbaugh et al., 2009b). To investigate the potential of the pregnancy-associated microbiota to promote inflammation, we transferred T1 and T3 microbiotas into female GF wild-type Swiss-Webster mice. T1 and T3 inocula were created from pooled samples derived from T1 and T3 samples of five healthy-weight women chosen at random without a priori knowledge of their microbial diversity profiles (these five were also used in the metagenomic analysis; Figure S5A). Posthoc 16S rRNA gene sequence analysis of the donor samples and pooled inocula revealed that the donors all exhibited a consistent shift in diversity that was also captured by the pooled inocula (Figure S5A). To verify that differences in T1 and T3 microbiotas observed in the donors were maintained in the recipient mice, we also sequenced 16S rRNA genes derived from mouse stool obtained 7 and 14 days posttransfer and from cecal samples obtained day 15. This analysis showed that the shift between T1 and T3 microbiotas observed in the donors (Figure S5A) was maintained in mice over the 2 week course of the experiment (Figures 6A, S6A, and S6B).

The transfer of specific gut microbiotas to otherwise healthy germ-free wild-type mice is sufficient to induce symptoms of metabolic syndrome, which, in addition to inflammation, include reduced insulin sensitivity and excess weight gain (Vijay-Kumar et al., 2010). Likewise, after 2 weeks, levels of inflammation markers were significantly higher overall in the stool and cecal samples from the T3 sample recipients compared to those of T1 recipients (ANOVA $p \leq 0.001$; Figures 6B and S6C–S6K and Table S5). Levels of lipocalin, which has recently been described as a sensitive marker of inflammation in mice (Carvalho et al., 2012), were also significantly higher in the T3 than T1 recipients (Table S5). Furthermore, we found that mouse recipients of the women's T1 microbiotas gained less adiposity compared to T3 recipients (37.9% $\pm$ 5.9% and 49.9% $\pm$ 4.4% for T1 and T3, respectively; $p = 0.06$, one-tailed t test; Figure 6C), despite similar food consumption. Levels of insulin were slightly lower in T1 than in T3 recipients after 2 weeks (0.266 $\pm$ 0.017 versus 0.281 $\pm$ 0.066 ng/ml, not significant [n.s.], respectively). Levels of blood glucose were slightly but significantly higher in T3 recipients after 30 min in an oral glucose

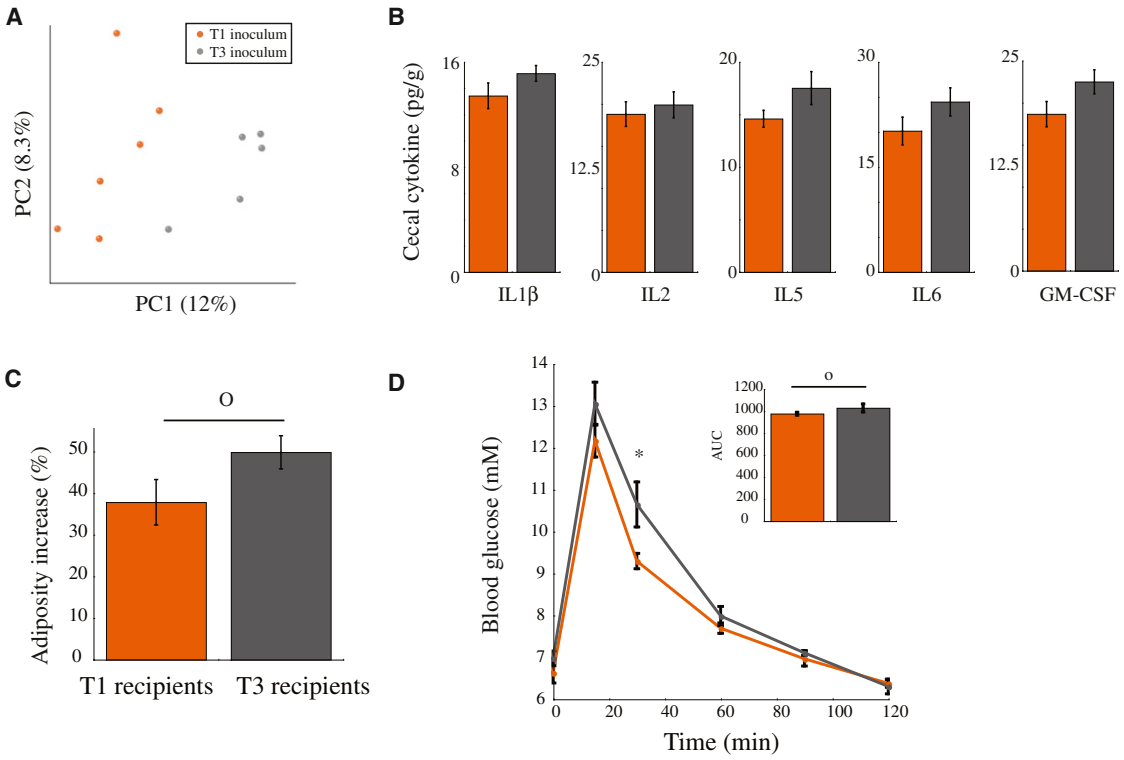

Figure 6. Transfer of T3 Microbiota to Germ-free Mice Causes Greater Metabolic Changes Than T1 Microbiota

Germ-free mice (11- to 13-weeks old) were intragastrically administered inoculum from T1 and T3 human donors (five mothers; fecal samples were pooled by trimester) and monitored for 2 weeks.

(A) Mouse cecal communities clustered based on PCoA of unweighted UniFrac matrix. Each sample corresponds to a mouse cecal microbiota harvested at 15 days and colored by trimester input. Variation explained by the principal coordinates is indicated on the axes.

(B) Cecal cytokine levels in recipient mice.

(C) Changes in adiposity (measured by DEXA) for mouse recipients of T1 (n = 6) and T3 (n = 5, one outlier removed) human gut microbiota.

(D) Blood glucose levels in recipient mice during oral glucose tolerance testing.

Data are mean ±SEM; o denotes $p < 0.1$; * denotes $p \leq 0.05$. See Figure S6.

tolerance test (Figure 6D). The observations that T3 recipients have reduced oral glucose tolerance, as well as greater inflammation and adiposity gains, than T1 recipients, together indicate that the T3 microbiota in particular has the capacity to induce metabolic changes in the host that resemble those occurring in both metabolic syndrome and pregnancy.

DISCUSSION

We describe a dramatic remodeling of the gut microbiota over the course of pregnancy. The first trimester gut microbiotas are similar to one another and comparable to those of normal healthy controls but shift substantially in phylogenetic composition and structure over the course of pregnancy. By the third trimester, the between-subject diversity has greatly expanded, even though within-subject diversity is reduced, and an enrichment of Proteobacteria and Actinobacteria is observed in a majority of T3 samples. Furthermore, the abundances of health-related bacteria are impacted. For instance, *Faecalibacterium*, which is a butyrate producer with anti-inflammatory effects that is depleted in inflammatory bowel disease (Sokol et al., 2008), is less abundant on average in T3. By the third trimester, each woman's microbiota has diverged in ways that could not be predicted from the T1 composition and that were not associated with health status or our diet records. Nonetheless, in the majority of women, the shift from T1 to T3 includes an increase in the abundance of Proteobacteria, which has been observed repeatedly for inflammation-associated dysbioses (Mukhopadhya et al., 2012).

One of the questions raised by the observation of greater interindividual bacterial diversity and the decrease in bacterial richness in T3 and 1 month postpartum is that an aberrant microbiota might colonize the baby and contribute negatively to the shaping of the immune system from birth, with long-term consequences for health problems, such as allergy development (van Nimwegen et al., 2011). Nevertheless, we found that, regardless of their age, the children's microbiotas were most similar to their mothers' microbiotas at T1, which may indicate that the taxa prevalent in T3 are at a selective disadvantage in the developing infant gut. Furthermore, we did not detect any differences between the microbiotas of GDM+ and GDM− mothers. We did observe an enrichment of *Streptococcus* in

T3 and in postpartum samples on average, and highest levels for children were in the gut microbiomes of the 1 month olds (although it should be noted that many members of the *Streptococcus* are commensal). Such enrichments may serve to educate the developing immune system to important members of the microbiota. As was recently reported for children on three continents (Yatsunenko et al., 2012), similarities between the child and mother microbiota increased with the age of the children, which underscores the importance of shared diet and environment on shaping the microbiota (Koenig et al., 2011).

Metabolic syndrome is a range of phenotypes that increase an individual's risk of developing type 2 diabetes, including hyperglycemia, insulin resistance, excess adiposity, and low-grade inflammation (Tilg and Moschen, 2006; Vijay-Kumar et al., 2010). Similarly, the latter stages of pregnancy have been described as a diabetogenic state that maintains hyperglycemia in the mother and a continuous supply of nutrients to the fetus. Gains in adiposity also prepare the female body for the energetic demands of lactation. Elevated levels of circulating proinflammatory cytokines have been reported for late pregnancy and have been correlated with levels of insulin resistance, suggesting a possible mechanistic link (Mor and Cardenas, 2010). The women in our study had reduced insulin sensitivity and increased circulating blood glucose levels and adiposity during gestation, and, in addition, we observed an increase in levels of inflammation markers in stool from T1 to T3. We suggest that a low-grade inflammation develops during pregnancy at the intestinal mucosal epithelium, and this inflammation may drive the microbial dysbiosis into a positive feedback loop with the altered host response (Lupp et al., 2007).

Two principal mechanisms have been proposed for how the gut microbiota can contribute to host adiposity: (1) increased energy extraction efficiency from the diet and (2) altered host-microbial interactions that promote metabolic inflammation. The results of our microbiota transfer experiments suggest that pregnancy is most similar to the second mechanism in which a dysbiosis drives changes in metabolism. Our results are very similar to the recently described mouse model for metabolic syndrome in which the microbiotas are sufficient and required to transfer aspects of metabolic syndrome to otherwise healthy germ-free wild-type recipient mice, including inflammation, excessive weight gain, hyperglycemia, and reduced insulin sensitivity (Vijay-Kumar et al., 2010).

The dysbiosis observed in T3 and the dysbiosis reported for the mouse model of metabolic syndrome (Carvalho et al., 2012; Vijay-Kumar et al., 2010) are also strikingly similar; both scenarios are characterized by elevated levels of Proteobacteria, greater between-individual variation, and excess bacterial load (described by Collado et al., 2008). Proteobacteria are active participants in inflammatory bowel disease (Mukhopadhya et al., 2012), and indeed, colonization with just one member of this group (*Escherichia coli*) is sufficient to induce macrophage infiltration into white adipose tissue and impaired glucose and insulin tolerance in GF mice (Caesar et al., 2012). Not all women showed elevated levels of Proteobacteria in T3, however, indicating that other factors, such as other members of the microbiota and potentially gene expression profiles, are also likely to be important for promoting inflammation. Although in the present study we pooled randomly selected donor microbiomes, comparison of individual donor effects on mouse phenotype will help identify the specific components of the microbiota driving metabolic inflammation. If the microbiotas are not only sufficient but also required for metabolic changes in pregnancy, these components should be widely shared among women with normal pregnancies and might share features with microbiomes of nonpregnant individuals of both sexes with metabolic syndrome.

It is interesting to note that some of the features of the T3 microbiota are similar to those of the obesity-associated microbiome shown to have enhanced energy extraction efficiency. For instance, both the low taxonomic richness and reduced metabolic network modularity that we observed in T3 have previously been reported for obese microbiomes (Greenblum et al., 2012; Qin et al., 2010; Turnbaugh et al., 2009a). In the T3 microbiome, the drivers of these traits are quite different from aspects of the obesity-associated microbiome. In the studies of obesity mentioned above, the microbiome is depleted in Bacteroidetes, such that gene categories related to simple sugar uptake, for instance, are overrepresented in obese compared to lean microbiomes. Furthermore, excess energy intake has been shown to favor Firmicutes over Bacteroidetes (Jumpertz et al., 2011), and in obesity, the microbiotas have been exposed long term to excess energy intake. In T3 versus T1, the relative abundances of Bacteroidetes and Firmicutes are largely unchanged, and we see no shift in the abundances of specific gene functional categories or metabolic pathways. Additionally, in stark contrast to the obese microbiome, the T3 microbiome is associated with a greater amount of energy lost in stool compared to T1. Thus, although some of the features of the microbiome are shared between the obese and T3 microbiotas, the underlying mechanisms by which they impact host adiposity can differ.

Conclusions

In summary, we have shown pregnancy to be associated with a profound alteration of the gut microbiota. The first trimester gut microbiota is similar in many aspects to that of healthy nonpregnant male and female controls, but by the third trimester, the structure and composition of the community resembles a disease-associated dysbiosis that differs among women. The underlying mechanisms resulting in the alteration of the microbiota remain to be clarified, but we speculate that the changes in the immune system at the mucosal surfaces in particular precipitate changes in the microbiota, although hormonal changes may also be important.

Dysbiosis, inflammation, and weight gain are features of metabolic syndrome, which increases the risk of type 2 diabetes in nonpregnant individuals. These same changes are central to normal pregnancy, where they may be highly beneficial, as they promote energy storage in fat tissue and provide for the growth of the fetus. Our work supports the emerging view that the gut microbiota affect host metabolism; however, the context (pregnant or not) defines how the outcome is interpreted (healthy or not). Metabolic changes are necessary to support a healthy pregnancy, which in itself is central to the fitness of a mammalian species. We hypothesize that, in mammalian reproductive biology, the host can manipulate the gut microbiota to promote

metabolic changes. Thus, the origins of host-microbial interactions that skew host metabolism toward greater insulin resistance, and which underlie much of the present-day obesity epidemic, may lie in reproductive biology.

EXPERIMENTAL PROCEDURES

Human Subjects and Data Collection

Enrollment of human subjects, collection of samples, and clinical and biometric data were described previously (Laitinen et al., 2009). Samples were collected as previously described (Collado et al., 2008, 2010).

Diversity and Phylogenetic Analyses

Bacterial 16S rRNA gene sequences (V1V2 region) were generated from PCR amplicons that were multiplexed and pyrosequenced, and data were analyzed by using the QIIME software package (Caporaso et al., 2010a) as described in Supplemental Information.

Comparison to the Human Microbiome Project Data

We combined our data with the recently released HMP 16S rRNA gene sequence data (Human Microbiome Project Consortium, 2012) and used a reference-based approach to pick OTUs at 97% ID by using the Greengenes latest release (McDonald et al., 2012). We compared β-diversity by using weighted UniFrac distances (Lozupone and Knight, 2005) calculated from the phylogenetic tree (Greengenes) after applying a rarefaction of 500 sequences/sample to standardize sequence counts.

Stool Energy Content

Gross energy content of paired T1 and T3 samples (20 mothers chosen at random) was determined by bomb calorimetry using an IKA C2000 basic calorimeter system (Dairy One, Ithaca, NY).

Shotgun Metagenomic Analysis of T1 and T3 Stool Samples

Samples from five mothers chosen randomly and the samples used as donors in the mouse transfer experiments were selected for shotgun metagenomic sequencing by using the Illumina HiSeq 2000. Sequence data were quality filtered and uploaded to MG-RAST. Taxonomy assignments (LCA), COG, and KEGG relative abundance data for protein-coding reads were summarized by using MG-RAST. Maximal information coefficient (MIC; Reshef et al., 2011) values were used to mine for between-COG ecological relationships within the two groups T1 and T3, accounting for linear as well as nonlinear relationships. A conservative cutoff of MIC = 1 was used to define between-COG edges in a network analysis of both T1 and T3 samples (MIC scores of 1 were well below $p = 0.05$ based on a Bonferroni correction). See Extended Experimental Procedures for details.

Microbiota Transfer Experiments

T1 and T3 stool samples from five women (age 24–30 years, normal prepregnancy BMIs) were used to colonize GF mice ($n = 6$ for T1 and $n = 6$ for T3). Adiposity was determined by DEXA as previously described (Bäckhed et al., 2004). Body weight and chow consumption were monitored weekly. Fecal pellets were collected at days 7 and 14. Oral glucose tolerance tests were performed by gavage with glucose (2 g/kg body weight) after a 4 hr fast. At day 15, mice were sacrificed after measurements of total body fat content by DEXA, plasma insulin was measured, and cecal content was removed. Body, gonadal white adipose tissue, and cecum weights were recorded for each mouse.

Statistical Analysis

Data are expressed as mean ±SEM. For complete statistical analysis methods, see Supplemental Information.

SUPPLEMENTAL INFORMATION

Supplemental Information includes Extended Experimental Procedures, one data file, six figures, and five tables and can be found with this article online at http://dx.doi.org/10.1016/j.cell.2012.07.008.

ACKNOWLEDGMENTS

We thank Mary-Claire King, Andrew Clark, and Andrew Gewirtz for their contributions to the manuscript, and we thank Daniel McDonlad and Nick Scalfone for technical assistance. This research was supported by The Hartwell Foundation, the NIH Human Microbiome Project DACC, the David and Lucile Packard Foundation, the Arnold and Mabel Beckman Foundation, the Cornell Center for Comparative Population Genomics, the Ragnar Söderberg Foundation, the Päivikki and Sakari Sohlberg Foundation, and the Academy of Finland.

Received: April 8, 2012
Revised: June 14, 2012
Accepted: July 5, 2012
Published: August 2, 2012

REFERENCES

Bäckhed, F., Ding, H., Wang, T., Hooper, L.V., Koh, G.Y., Nagy, A., Semenkovich, C.F., and Gordon, J.I. (2004). The gut microbiota as an environmental factor that regulates fat storage. Proc. Natl. Acad. Sci. USA *101*, 15718–15723.

Barbour, L.A., McCurdy, C.E., Hernandez, T.L., Kirwan, J.P., Catalano, P.M., and Friedman, J.E. (2007). Cellular mechanisms for insulin resistance in normal pregnancy and gestational diabetes. Diabetes Care *30* (*Suppl 2*), S112–S119.

Beigi, R.H., Yudin, M.H., Cosentino, L., Meyn, L.A., and Hillier, S.L. (2007). Cytokines, pregnancy, and bacterial vaginosis: comparison of levels of cervical cytokines in pregnant and nonpregnant women with bacterial vaginosis. J. Infect. Dis. *196*, 1355–1360.

Caesar, R., Reigstad, C.S., Bäckhed, H.K., Reinhardt, C., Ketonen, M., Ostergren Lundén, G., Cani, P.D., and Bäckhed, F. (2012). Gut-derived lipopolysaccharide augments adipose macrophage accumulation but is not essential for impaired glucose or insulin tolerance in mice. Gut. Published online April 25, 2012. http://dx.doi.org/10.1136/gutjnl-2011-301689.

Cani, P.D., Amar, J., Iglesias, M.A., Poggi, M., Knauf, C., Bastelica, D., Neyrinck, A.M., Fava, F., Tuohy, K.M., Chabo, C., et al. (2007). Metabolic endotoxemia initiates obesity and insulin resistance. Diabetes *56*, 1761–1772.

Caporaso, J.G., Kuczynski, J., Stombaugh, J., Bittinger, K., Bushman, F.D., Costello, E.K., Fierer, N., Peña, A.G., Goodrich, J.K., Gordon, J.I., et al. (2010a). QIIME allows analysis of high-throughput community sequencing data. Nat. Methods *7*, 335–336.

Carvalho, F.A., Koren, O., Johansson, M., Nalbantoglu, I., Aitken, J.D., Su, Y., Walters, W.A., González Peña, A., Clemente, J.C., Barnich, N., et al. (2012). Inability to manage Proteobacteria drives colitis in T5KO mice. Cell Host Microbe. Published online August 2, 2012. http://dx.doi.org/10.1016/j.chom.2012.07.004.

Collado, M.C., Isolauri, E., Laitinen, K., and Salminen, S. (2008). Distinct composition of gut microbiota during pregnancy in overweight and normal-weight women. Am. J. Clin. Nutr. *88*, 894–899.

Collado, M.C., Isolauri, E., Laitinen, K., and Salminen, S. (2010). Effect of mother's weight on infant's microbiota acquisition, composition, and activity during early infancy: a prospective follow-up study initiated in early pregnancy. Am. J. Clin. Nutr. *92*, 1023–1030.

De Filippo, C., Cavalieri, D., Di Paola, M., Ramazzotti, M., Poullet, J.B., Massart, S., Collini, S., Pieraccini, G., and Lionetti, P. (2010). Impact of diet in shaping gut microbiota revealed by a comparative study in children from Europe and rural Africa. Proc. Natl. Acad. Sci. USA *107*, 14691–14696.

Di Cianni, G., Miccoli, R., Volpe, L., Lencioni, C., and Del Prato, S. (2003). Intermediate metabolism in normal pregnancy and in gestational diabetes. Diabetes Metab. Res. Rev. *19*, 259–270.

Greenblum, S., Turnbaugh, P.J., and Borenstein, E. (2012). Metagenomic systems biology of the human gut microbiome reveals topological shifts associated with obesity and inflammatory bowel disease. Proc. Natl. Acad. Sci. USA *109*, 594–599.

Gregor, M.F., and Hotamisligil, G.S. (2011). Inflammatory mechanisms in obesity. Annu. Rev. Immunol. *29*, 415–445.

Human Microbiome Project Consortium. (2012). Structure, function and diversity of the healthy human microbiome. Nature *486*, 207–214.

Jumpertz, R., Le, D.S., Turnbaugh, P.J., Trinidad, C., Bogardus, C., Gordon, J.I., and Krakoff, J. (2011). Energy-balance studies reveal associations between gut microbes, caloric load, and nutrient absorption in humans. Am. J. Clin. Nutr. *94*, 58–65.

Kirwan, J.P., Hauguel-De Mouzon, S., Lepercq, J., Challier, J.C., Huston-Presley, L., Friedman, J.E., Kalhan, S.C., and Catalano, P.M. (2002). TNF-alpha is a predictor of insulin resistance in human pregnancy. Diabetes *51*, 2207–2213.

Koenig, J.E., Spor, A., Scalfone, N., Fricker, A.D., Stombaugh, J., Knight, R., Angenent, L.T., and Ley, R.E. (2011). Succession of microbial consortia in the developing infant gut microbiome. Proc. Natl. Acad. Sci. USA *108* (*Suppl 1*), 4578–4585.

Kuczynski, J., Lauber, C.L., Walters, W.A., Parfrey, L.W., Clemente, J.C., Gevers, D., and Knight, R. (2012). Experimental and analytical tools for studying the human microbiome. Nat. Rev. Genet. *13*, 47–58.

Lain, K.Y., and Catalano, P.M. (2007). Metabolic changes in pregnancy. Clin. Obstet. Gynecol. *50*, 938–948.

Laitinen, K., Poussa, T., and Isolauri, E.; Nutrition, Allergy, Mucosal Immunology and Intestinal Microbiota Group. (2009). Probiotics and dietary counselling contribute to glucose regulation during and after pregnancy: a randomised controlled trial. Br. J. Nutr. *101*, 1679–1687.

Ley, R.E., Bäckhed, F., Turnbaugh, P., Lozupone, C.A., Knight, R.D., and Gordon, J.I. (2005). Obesity alters gut microbial ecology. Proc. Natl. Acad. Sci. USA *102*, 11070–11075.

Lozupone, C., and Knight, R. (2005). UniFrac: a new phylogenetic method for comparing microbial communities. Appl. Environ. Microbiol. *71*, 8228–8235.

Lupp, C., Robertson, M.L., Wickham, M.E., Sekirov, I., Champion, O.L., Gaynor, E.C., and Finlay, B.B. (2007). Host-mediated inflammation disrupts the intestinal microbiota and promotes the overgrowth of Enterobacteriaceae. Cell Host Microbe *2*, 119–129.

McDonald, D., Price, M.N., Goodrich, J., Nawrocki, E.P., DeSantis, T.Z., Probst, A., Andersen, G.L., Knight, R., and Hugenholtz, P. (2012). An improved Greengenes taxonomy with explicit ranks for ecological and evolutionary analyses of bacteria and archaea. ISME J. *6*, 610–618.

Mor, G., and Cardenas, I. (2010). The immune system in pregnancy: a unique complexity. Am. J. Reprod. Immunol. *63*, 425–433.

Mukhopadhya, I., Hansen, R., El-Omar, E.M., and Hold, G.L. (2012). IBD-what role do Proteobacteria play? Nat. Rev. Gastroenterol. Hepatol. *9*, 219–230.

Nelson, S.M., Matthews, P., and Poston, L. (2010). Maternal metabolism and obesity: modifiable determinants of pregnancy outcome. Hum. Reprod. Update *16*, 255–275.

Newbern, D., and Freemark, M. (2011). Placental hormones and the control of maternal metabolism and fetal growth. Curr. Opin. Endocrinol. Diabetes Obes. *18*, 409–416.

Palmer, C., Bik, E.M., DiGiulio, D.B., Relman, D.A., and Brown, P.O. (2007). Development of the human infant intestinal microbiota. PLoS Biol. *5*, e177.

Qin, J., Li, R., Raes, J., Arumugam, M., Burgdorf, K.S., Manichanh, C., Nielsen, T., Pons, N., Levenez, F., Yamada, T., et al.; MetaHIT Consortium. (2010). A human gut microbial gene catalogue established by metagenomic sequencing. Nature *464*, 59–65.

Reshef, D.N., Reshef, Y.A., Finucane, H.K., Grossman, S.R., McVean, G., Turnbaugh, P.J., Lander, E.S., Mitzenmacher, M., and Sabeti, P.C. (2011). Detecting novel associations in large data sets. Science *334*, 1518–1524.

Saiki, T., Mitsuyama, K., Toyonaga, A., Ishida, H., and Tanikawa, K. (1998). Detection of pro- and anti-inflammatory cytokines in stools of patients with inflammatory bowel disease. Scand. J. Gastroenterol. *33*, 616–622.

Salzman, N.H., Hung, K., Haribhai, D., Chu, H., Karlsson-Sjöberg, J., Amir, E., Teggatz, P., Barman, M., Hayward, M., Eastwood, D., et al. (2010). Enteric defensins are essential regulators of intestinal microbial ecology. Nat. Immunol. *11*, 76–83.

Sim, K., Cox, M.J., Wopereis, H., Martin, R., Knol, J., Li, M.S., Cookson, W.O., Moffatt, M.F., and Kroll, J.S. (2012). Improved detection of bifidobacteria with optimised 16S rRNA-gene based pyrosequencing. PLoS ONE *7*, e32543.

Slack, E., Hapfelmeier, S., Stecher, B., Velykoredko, Y., Stoel, M., Lawson, M.A., Geuking, M.B., Beutler, B., Tedder, T.F., Hardt, W.D., et al. (2009). Innate and adaptive immunity cooperate flexibly to maintain host-microbiota mutualism. Science *325*, 617–620.

Sokol, H., Pigneur, B., Watterlot, L., Lakhdari, O., Bermudez-Humaran, L.G., Gratadoux, J.J., Blugeon, S., Bridonneau, C., Furet, J.P., Corthier, G., et al. (2008). Faecalibacterium prausnitzii is an anti-inflammatory commensal bacterium identified by gut microbiota analysis of Crohn disease patients. Proc. Natl. Acad. Sci. USA *105*, 16731–16736.

Spor, A., Koren, O., and Ley, R. (2011). Unravelling the effects of the environment and host genotype on the gut microbiome. Nat. Rev. Microbiol. *9*, 279–290.

Straka, M. (2011). Pregnancy and periodontal tissues. Neuroendocrinol. Lett. *32*, 34–38.

Tilg, H., and Moschen, A.R. (2006). Adipocytokines: mediators linking adipose tissue, inflammation and immunity. Nat. Rev. Immunol. *6*, 772–783.

Turnbaugh, P.J., Ley, R.E., Mahowald, M.A., Magrini, V., Mardis, E.R., and Gordon, J.I. (2006). An obesity-associated gut microbiome with increased capacity for energy harvest. Nature *444*, 1027–1031.

Turnbaugh, P.J., Hamady, M., Yatsunenko, T., Cantarel, B.L., Duncan, A., Ley, R.E., Sogin, M.L., Jones, W.J., Roe, B.A., Affourtit, J.P., et al. (2009a). A core gut microbiome in obese and lean twins. Nature *457*, 480–484.

Turnbaugh, P.J., Ridaura, V.K., Faith, J.J., Rey, F.E., Knight, R., and Gordon, J.I. (2009b). The effect of diet on the human gut microbiome: a metagenomic analysis in humanized gnotobiotic mice. Sci. Transl. Med. *1*, 6ra14.

van Nimwegen, F.A., Penders, J., Stobberingh, E.E., Postma, D.S., Koppelman, G.H., Kerkhof, M., Reijmerink, N.E., Dompeling, E., van den Brandt, P.A., Ferreira, I., et al. (2011). Mode and place of delivery, gastrointestinal microbiota, and their influence on asthma and atopy. J. Allergy Clin. Immunol. *128*, 948, 955.e3.

Vijay-Kumar, M., Aitken, J.D., Carvalho, F.A., Cullender, T.C., Mwangi, S., Srinivasan, S., Sitaraman, S.V., Knight, R., Ley, R.E., and Gewirtz, A.T. (2010). Metabolic syndrome and altered gut microbiota in mice lacking Toll-like receptor 5. Science *328*, 228–231.

Wu, G.D., Chen, J., Hoffmann, C., Bittinger, K., Chen, Y.Y., Keilbaugh, S.A., Bewtra, M., Knights, D., Walters, W.A., Knight, R., et al. (2011). Linking long-term dietary patterns with gut microbial enterotypes. Science *334*, 105–108.

Yatsunenko, T., Rey, F.E., Manary, M.J., Trehan, I., Dominguez-Bello, M.G., Contreras, M., Magris, M., Hidalgo, G., Baldassano, R.N., Anokhin, A.P., et al. (2012). Human gut microbiome viewed across age and geography. Nature *486*, 222–227.

EXTENDED EXPERIMENTAL PROCEDURES

Human Subjects

The women studied here were participants in a previous clinical study of nutrition in pregnancy, which included the collection of stool, and visits to the University of Turku, at which time dietary records and other biometric/clinical data were obtained (Laitinen et al., 2009; Collado et al., 2008, 2010). Enrollment of human subjects, and collection of samples, clinical and biometric data were described previously (Laitinen et al., 2009). Clinical and biometric data are summarized in Tables 1 and S1. Additionally, sixteen women took probiotics during their pregnancies (*Bifidobacterium lactis* and *Lactobacillus rhamnosus* (10^{10} CFU/day of each in capsule form). Seven women studied here took antibiotics during the study: 2 during the first trimester, and 5 during the second trimester, but none during the third trimester (one of the second trimester antibiotic-users subsequently was dropped from the analysis due to low sequence counts, see below). The pregnancies studied here were the first for 54% of the women, second for 29%, third for 11% and fourth for 6%. Written informed consent was obtained from the participants, and the study protocol was approved by the Ethics Committee of the Hospital District of South-West Finland (registration number NCT00167700). The stool microbiome study was approved by the Cornell University Institutional Review Board.

Sample Handling and DNA Extraction

Stool samples were collected as previously described (Collado et al., 2008, 2010). Samples were frozen at −18°C following collection at home, delivered frozen to the University of Turku during the study visits and maintained frozen at −80°C. After shipping to Cornell University on dry ice, each sample was lyophilized, then finely ground and homogenized by roller-milling. Roller-milling was accomplished by inserting steel rods (1x6 or 2x3 mm diameter x 10 cm length) into 50 ml conical tubes containing the freeze-dried samples, and tumbling the tubes for 12-24 hr in a rotary tumbler (Covington) at room temperature. DNA was isolated from ~0.1 g of each freeze-dried, homogenized sample using the PowerSoil-htp DNA isolation kit as described by the manufacturer (MoBio Laboratories Ltd, Carlsbad, CA) with a beadbeater (BioSpec, Bartlesville, OK) set on high for 2 min. Bacterial 16S rRNA gene sequences were PCR-amplified from each sample using the 27F and 338R primers for the V1V2 hypervariable region of the 16S rRNA gene as previously described (Koren et al., 2011). Primers included unique error-correcting 12-base barcodes used to tag PCR products from different samples (Hamady et al., 2008). PCR reactions consisted of 2.5U Easy-A high-fidelity enzyme and 1X buffer (Stratagene, La Jolla, CA), 0.2 μM of each primer, 10-100 ng DNA template; reaction conditions consisted of an initial denaturing step for 2 min at 95°C, followed by 30 cycles of 40 s at 95°C, 30 s at 57°C and 60 s at 72°C. Triplicate PCR reactions were performed for each sample, combined and then purified with Ampure magnetic purification beads (Agencourt, Danvers, MA). Purified PCR products were quantified using a Quant-iT PicoGreen dsDNA assay (Invitrogen, Carlsbad, CA). The pooled products were sequenced at Engencore (University of South Carolina) using Roche 454 FLX and Titanium chemistry.

16S rRNA Gene Sequence Analysis

For quality filtering the raw data we discarded sequences < 200 bp or > 1,000 bp, and sequences containing primer mismatches, uncorrectable barcodes, ambiguous bases, or homopolymer runs in excess of 6 bases. The sequences that passed the quality filters were analyzed using the QIIME software package (Caporaso et al., 2010a). Sequences were checked for chimeras using UCHIME and assigned to operational taxonomic units (OTUs) using OTUpipe (Edgar et al., 2011) with a 97% threshold of pairwise identity, and then classified taxonomically using the Greengenes (GG) reference database and a confidence threshold of 60% (McDonald et al., 2012). (Note that for Figure 2B, the confidence for the taxonomic assignments was set to 80%.) The GG taxonomies were used to generate summaries of the taxonomic distributions of OTUs across different levels (phylum, order, family, genus; see Data S1). To standardize sequence counts across samples with uneven sampling, we randomly selected 790 sequences per sample (rarefaction) and used this as a basis to compare abundances of OTUs across samples. For phylogenetic tree-based analyses, each OTU was represented by a single sequence that was aligned using PyNAST (Caporaso et al., 2010b). A phylogenetic tree was built with FastTree (Price et al., 2009) and used for estimates of α-diversity (within sample diversity, using Faith's phylogenetic diversity [PD; Faith, 1992]) and β-diversity (between sample diversity, using unweighted and weighted UniFrac (Lozupone and Knight, 2005). We measured community evenness using the Gini coefficient (Wittebolle et al., 2009). For both PD measurements and Gini coefficients, means and standard errors for given categories were calculated from 100 iterations using a rarefaction of 790 sequences per sample.

The nearest shrunken centroid method (Knights et al., 2011; Tibshirani et al., 2002) was used to identify OTUs that were specifically over (or under)-represented in a given category (i.e., T1 or T3). The threshold for attribute selection was chosen in order to minimize the overall misclassification error. The analysis was performed using the Predictive Analysis of Microarrays (PAM) package under the R software.

Comparison to the Human Microbiome Project Data

We combined the recently released HMP 16S rRNA gene sequences data (V1V2 and V3V5 regions; Human Microbiome Project Consortium [2012]) with our 16S rRNA gene sequence data (V1V2) and used a reference-based approach to pick OTUs at 97%ID using the GG latest release (McDonald et al., 2012). We compared β-diversity using weighted UniFrac distances (Lozupone and Knight, 2005) calculated from the phylogenetic tree (GG release), after applying a rarefaction of 500 sequences/sample to standardize sequence counts between data sets.

Statistical Analysis of the OTU Abundances and Covariates

To search for associations between the metadata (diet records, antibiotic use, probiotic use, and clinical data, Table 1) and the abundances of the OTUs (summarized at different taxonomic levels), we employed Spearman rank correlations for the continuous metadata and ANOVA for the categorical metadata. We corrected for multiple comparisons using a false discovery rate (FDR) of 0.05. We compared the magnitude of change from T1 to T3 for each OTU in all the mothers to differences in the means for clinical and diet data categories. We also used MINE statistics (Reshef et al., 2011) to determine non-linear (MIC-$\rho^2 > 0.2$) relationships between OTUs (''noncoexistence''). To test if these non-linear relationships could be explained by the categorical metadata, we used the heuristic *A* as described by Reshef et al. (2011).

Comparisons of Microbiotas between Mothers and Infants

We compared mothers' microbiotas at T1, T3, and 1 month postpartum to the infant samples. For mother-infant pairs, mothers' microbiotas were not more similar to their own child's microbiota than to unrelated children's microbiota (using weighted and unweighted UniFrac). PAM-R analysis of genus-level OTUs did not reveal OTUs that could discriminate between different ages (1 month, 6 months, and 4 years). Spearman correlation analysis of OTU abundances between mothers at T1 and T3 to their own babies at 1 month of age did not reveal any significant correlations.

Influence of Diet on the Microbiome

A previous study of diet effects on the gut microbiome reported significant correlations between diet composition and OTU abundances (Wu et al., 2011). We first searched for associations between our diet records and genus-level OTU abundances. To be consistent with Wu et al., we implemented their methods: Spearman correlations were calculated for all genera found in more than 10% of the samples. We tested each trimester independently, in order to remove bias that might be a result of the major effect of trimester, yet found no significant associations between OTU abundances and diet records at either trimester, using both an FDR of 0.05, or the much more permissive FDR of 0.25 used by Wu et al. (2011). Additionally, we examined OTUs at higher taxonomic levels, but no significant associations between taxonomic abundances and our diet records were found.

Associations between the UniFrac Distances and the Clinical and Diet Data

To gauge whether diet or health data could be related to the degree of change in diversity within an individual from T1 to T3, we searched for significant associations between host-related data (Table 1) and the weighted and unweighted UniFrac distances between T3 and T1 samples within individuals. ANOVA was used for the categorical covariates and linear regression was performed on the Box-Cox normalized continuous covariates using the command PowerTransfom command implemented in the R package ''car.'' No significant associations were found (using an FDR of 0.05).

Enterotypes

We searched our data for enterotypes using previously described methods (Arumugam et al., 2011; Wu et al., 2011). We calculated the silhouette widths (Rousseeuw, 1987) for weighted and unweighted UniFrac distances for each trimester separately. (Note that the T1 and T3 samples form strong clusters, but a shift in composition over time should not be interpreted as enterotypes). The silhouette widths for T1 and T3 (unweighted UniFrac) were 0.01 and 0.04, respectively, and 0.2 and 0.47 for the weighted UniFrac distances for T1 and T3. Since Silhouette indices smaller than 0.5 are considered weak and could be artificial (Rousseeuw, 1987) we concluded that enterotypes were not present in our data sets.

Effect of Sample Handling Method on 16S rRNA Gene Sequence Analysis

To assess the effect of method of sample storage and handling samples (i.e, frozen at −80°C or frozen at −80°C then freeze-dried and ground) on the phylogenetic composition of T1 samples (i.e., the shift along PC1, Figure 3), we generated 16S rRNA gene sequence data from a set of samples handled the 2 different ways. The DNA was extracted, amplified and analyzed as described above. No significant differences between mean OTU abundances between handling treatments were found using paired t tests (FDR, 0.05) for OTUs at any of the taxonomic levels.

Shotgun Metagenomic Analysis of T1 and T3 Stool Samples

Samples from 5 mothers selected randomly, and the samples used in the mouse transfer experiments (5 healthy mothers chosen at random) were subjected to shotgun metagenomic analysis. Samples were sequenced at the Cornell University and Columbia University sequencing centers using an Illumina HiSeq2000. Read counts are summarized in Table S3.

Sequences were quality filtered (trimmed ends at quality scores with code ''B'' or any ambiguous base, followed by discarding any reads with less than 75 bp) and uploaded to MG-RAST (Meyer et al., 2008) with the default quality filtering and identical read dereplication (see Table S3). Taxonomy assignments (LCA) and COG relative abundance data for protein-coding reads were summarized using MG-RAST (e-value $< 10^{-5}$; ID > 50%; alignment length > 20 aa). Maximal information coefficient (MIC; Reshef et al., 2011) values were used to mine for between-COG ecological relationships within the two groups T1 and T3, accounting for linear as well as non-linear relationships. A conservative cutoff of MIC = 1 was used to define between-COG edges in a network analysis of both T1 and T3 (MIC scores of 1 were well below p = 0.05 based on a Bonferroni correction). We included 1,392 COGs as attributes in this

MIC/network analysis, based on applying occurrence cutoffs in > 75% of samples and > 0.01% relative abundance in at least one sample (abundance in IDed COG pool, not the overall set of sample reads). Networks were imported into Cytoscape 2.8, which was used for visualization and to calculate network statistics.

KEGG gene categories in Figure 5A are as follows: [1.1] Metabolism;Carbohydrate Metabolism; [1.2] Metabolism;Energy Metabolism; [1.3] Metabolism;Lipid Metabolism; [1.4] Metabolism;Nucleotide Metabolism; [1.5] Metabolism;Amino Acid Metabolism; [1.6] Metabolism;Metabolism of Other Amino Acids; [1.7] Metabolism;Glycan Biosynthesis and Metabolism; [1.8] Metabolism;Metabolism of Cofactors and Vitamins; [1.9] Metabolism;Metabolism of Terpenoids and Polyketides; [1.10] Metabolism;Biosynthesis of Other Secondary Metabolites; [1.11] Metabolism;Xenobiotics Biodegradation and Metabolism; [2.1] Genetic Information Processing;Transcription; [2.2] Genetic Information Processing;Translation; [2.3] Genetic Information Processing;Folding, Sorting and Degradation; [2.4] Genetic Information Processing;Replication and Repair; [3.1] Environmental Information Processing;Membrane Transport; [3.2] Environmental Information Processing;Signal Transduction; [4.3] Cellular Processes;Cell Growth and Death.

Cytokine Analysis for Human Stool

Aliquots (50 mg) of feces were re-suspended in PBS containing 1% BSA (Sigma) to achieve a concentration of 100 μg/ml and homogenized for 30 s using a Mini-Beadbeater-24 (Biospec). Samples were then centrifuged for 1 min at 5,000 g, and the supernatant was used for cytokine analysis. Cytokines were quantified using the Bio-Plex Pro Cytokine 8-Plex Assay kit coupled with the Bio-Plex 200 (Bio-Rad). We used the following fixed-effect ANOVA model to study the variation in cytokine levels between T1 and T3:

$$Y_{ijkl} = \text{cytokine}_i + \text{trimester}_j + \text{cytokine} * \text{trimester}_{ij} + \varepsilon_{ijkl}$$

where *cytokine* is the type of cytokine (i = 1, …, 8), *trimester* is stage of pregnancy (j = 1, 2 for T1 or T3, respectively) and *cytokine*trimester* tests an interaction effect. Data were log-transformed prior to the ANOVA to achieve normality and homogeneity of the residuals (ε_{ijk}) distribution. Tukey HSD tests were performed to assess significant pair-wise differences.

Microbiota Transfer Experiments

All experiments involving mice were performed using protocols approved by the local animal ethics committee at the University of Gothenburg, Sweden. Eleven to 13-week-old germ-free (GF) female Swiss Webster mice were maintained in flexible film isolators under a strict 12L:12D 24 hr cycle. GF status was verified regularly by anaerobic culturing in addition to PCR for bacterial 16*S* rRNA (Reigstad et al., 2009). Mice were fed autoclaved chow diet (Labdiet) *ad libitum*. T1 and T3 stool samples from five women (age 24-30 years, normal pre-pregnancy BMIs) were used to colonize GF mice. Due to concerns that freeze-drying could impact the viability of the microbiota, the donor samples were selected in Finland (without *a priori* knowledge of bacterial diversity) and sent frozen to the University of Gothenburg. Handling of human fecal samples was performed under anaerobic conditions. Each fecal sample (0.1 g) was suspended in 1.5 ml of reduced sterile PBS, and T1/T3 pools were made from equal volume of donor suspensions. The pooled inoculum samples were vortexed for 5 min followed by sedimentation for 5 min to allow bigger particles to settle to the bottom of the tube. Adiposity was determined by DEXA as previously described (Bäckhed et al., 2004). Mice were divided into two groups with equal contents of total body fat and were then immediately gavaged with 200 μl of the T1 (n = 6) or T3 suspension (n = 6), placed in ventilated cages and studied for 2 weeks. One mouse inoculated with T3 microbiota failed to gain any weight and was excluded from further analysis.

Body weight and chow consumption were monitored weekly. Food was weighed at the beginning of the experiment and after 7 and 14 days. On these days fecal pellets were also collected, snap frozen in liquid N_2 and stored at −80°C. At day 14, oral glucose tolerance tests were performed by gavage with glucose (2 g/kg body weight) after a 4 hr fast. Tail blood samples were collected at −30, 0, 15, 30, 60, 90, and 120 min and blood glucose levels were determined. At day 15, mice were sacrificed after measurements of total body fat content by DEXA. Cecal content was removed, snap frozen in liquid N_2 and stored at −80°C. Body, gonadal white adipose tissue and cecum weights were recorded for each mouse. Insulin levels were measured from blood collected from the vena cava at sacrifice, using an Ultra Sensitive Mouse Insulin ELISA Kit (Crystal Chem Inc, Downers Grove, IL, USA).

Mouse Fecal and Cecal Cytokine Analysis

Cytokines in mouse fecal and cecal samples were performed as described above, but using the mouse cytokine version of the kit, and additional IL-6 antibodies and magnetic beads were included. We used the R&D DuoSet ELISA system (R&D Systems) to measure lipocalin (Carvalho et al., 2012). We applied the following fixed-effect ANOVA model to study the variation in cytokine levels over the time course and between mice inoculated with T1 and T3 samples:

$$Y_{ijkl} = \text{cytokine}_i + \text{inoculum}_j + \text{week}_k + \text{cytokine} * \text{inoculum}_{ij} + \text{cytokine} * \text{week}_{ik} + \text{inoculum} * \text{week}_{jk} + \varepsilon_{ijkl}$$

where *cytokine* is the type of cytokine (i = 1, …, 9), *inoculum* is whether the mice were inoculated with T1 or T3 fecal samples (j = 1, 2), *week* is the week during which the samples were taken (k = 1, 2, 3) and *cytokine*inoculum*, *cytokine*week* and *inoculums*week* test for interaction effects. Data were log-transformed prior to the ANOVA to achieve normality and homogeneity of the residuals (ε_{ijkl}) distribution.

Mouse Fecal and Cecal Bacterial Diversity

DNA was extracted from frozen mouse cecal and fecal pellets and 16S rRNA gene sequences were derived as described for human stool samples above.

SUPPLEMENTAL REFERENCES

Arumugam, M., Raes, J., Pelletier, E., Le Paslier, D., Yamada, T., Mende, D.R., Fernandes, G.R., Tap, J., Bruls, T., Batto, J.M., et al.; MetaHIT Consortium (2011). Enterotypes of the human gut microbiome. Nature *473*, 174–180.

Caporaso, J.G., Bittinger, K., Bushman, F.D., DeSantis, T.Z., Andersen, G.L., and Knight, R. (2010b). PyNAST: a flexible tool for aligning sequences to a template alignment. Bioinformatics *26*, 266–267.

Edgar, R.C., Haas, B.J., Clemente, J.C., Quince, C., and Knight, R. (2011). UCHIME improves sensitivity and speed of chimera detection. Bioinformatics *27*, 2194–2200.

Faith, D.P. (1992). Conservation evaluation and phylogenetic diversity. Biol. Conserv. *61*, 1–10.

Hamady, M., Walker, J.J., Harris, J.K., Gold, N.J., and Knight, R. (2008). Error-correcting barcoded primers for pyrosequencing hundreds of samples in multiplex. Nat. Methods *5*, 235–237.

Knights, D., Kuczynski, J., Koren, O., Ley, R.E., Field, D., Knight, R., DeSantis, T.Z., and Kelley, S.T. (2011). Supervised classification of microbiota mitigates mislabeling errors. ISME J. *5*, 570–573.

Koren, O., Spor, A., Felin, J., Fåk, F., Stombaugh, J., Tremaroli, V., Behre, C.J., Knight, R., Fagerberg, B., Ley, R.E., and Bäckhed, F. (2011). Human oral, gut, and plaque microbiota in patients with atherosclerosis. Proc. Natl. Acad. Sci. USA *108* (*Suppl 1*), 4592–4598.

Meyer, F., Paarmann, D., D'Souza, M., Olson, R., Glass, E.M., Kubal, M., Paczian, T., Rodriguez, A., Stevens, R., Wilke, A., et al. (2008). The metagenomics RAST server - a public resource for the automatic phylogenetic and functional analysis of metagenomes. BMC Bioinformatics *9*, 386.

Price, M.N., Dehal, P.S., and Arkin, A.P. (2009). FastTree: computing large minimum evolution trees with profiles instead of a distance matrix. Mol. Biol. Evol. *26*, 1641–1650.

Reigstad, C.S., Lundén, G.O., Felin, J., and Bäckhed, F. (2009). Regulation of serum amyloid A3 (SAA3) in mouse colonic epithelium and adipose tissue by the intestinal microbiota. PLoS ONE *4*, e5842.

Rousseeuw, P. (1987). Silhouettes: a graphical aid to the interpretation and validation of cluster-analysis. J. Comput. Appl. Math. *20*, 53–65.

Tibshirani, R., Hastie, T., Narasimhan, B., and Chu, G. (2002). Diagnosis of multiple cancer types by shrunken centroids of gene expression. Proc. Natl. Acad. Sci. USA *99*, 6567–6572.

Wittebolle, L., Marzorati, M., Clement, L., Balloi, A., Daffonchio, D., Heylen, K., De Vos, P., Verstraete, W., and Boon, N. (2009). Initial community evenness favours functionality under selective stress. Nature *458*, 623–626.

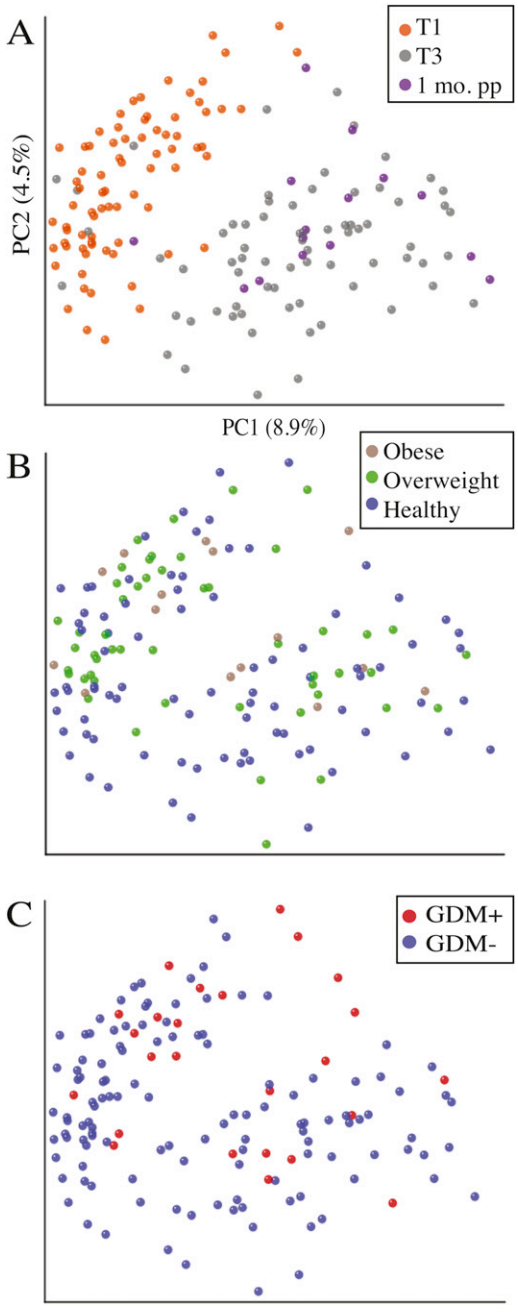

Figure S1. 16S rRNA Gene Surveys Reveal Changes to Microbial Diversity during Pregnancy, Related to Figure 1

(A–C) Microbial communities clustered using PCoA of the unweighted UniFrac matrix. The percentage of variation explained by the principal coordinates is indicated on the axes. Each point corresponds to a community colored by (A) time of collection (T1, T3, or 1 month postpartum); (B) pre-pregnancy BMI (obese, overweight or healthy); (C) gestational diabetes status (GDM+ and GDM−).

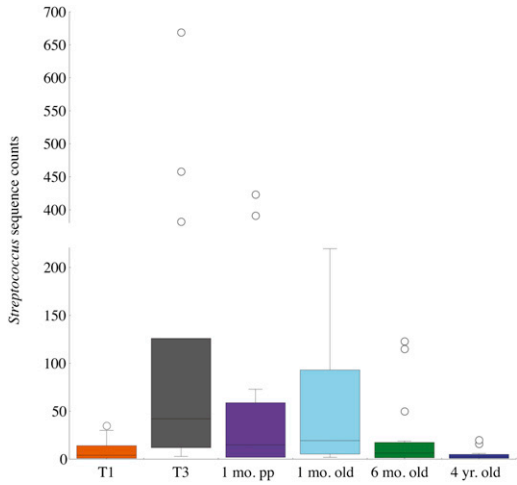

Figure S2. Relative Abundance of the *Streptococcus* Genus in Fecal Microbiotas of Women and Their Children, Related to Figure 2
Boxplots for counts of all OTUs classified as belonging to the *Streptococcus* genus (rarefied at 790 randomly selected sequences/sample).

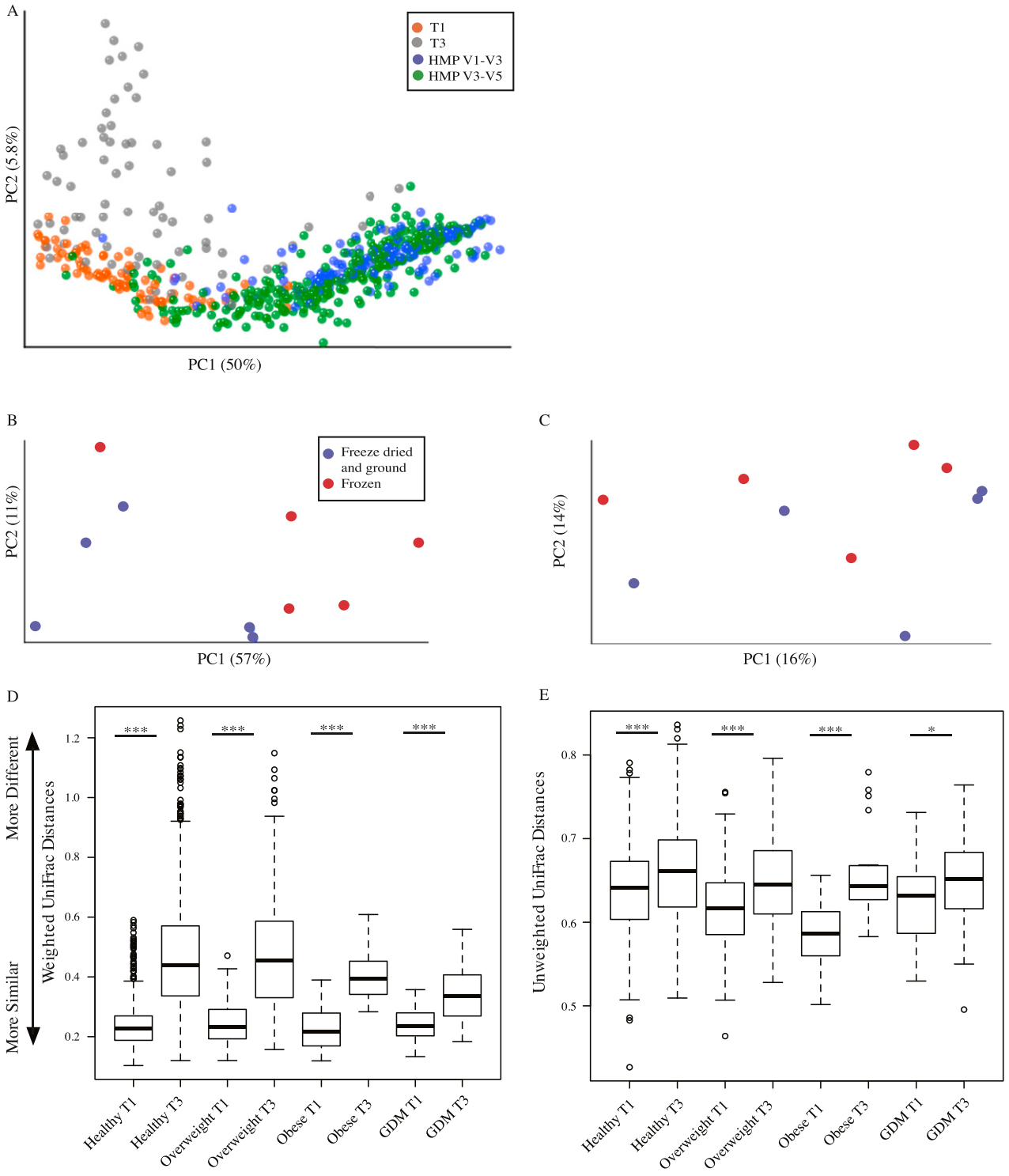

Figure S3. Factors Influencing β-Diversity, Related to Figure 3

(A) Effect of primer region. PCoA of the weighted UniFrac distances between T1 (orange), T3 (gray), normal healthy HMP V1V3 data set (blue) and V3V5 data set (green).

(B and C) Effect of sample handling. A set of samples were either freeze-dried and ground (blue, as described in Experimental Procedures) or simply frozen (red, HMP protocol) prior to DNA extraction. Both weighted (B) and unweighted (C) UniFrac analyses are shown. For details see legend of Figure 1.

(D and E) Effects of pre-pregnancy BMI and GDM status. Box plots showing mean weighted (D) and unweighted (E) UniFrac distances for T1 and T3 samples, for the pre-pregnancy healthy, pre-pregnancy overweight, pre-pregnancy obese and GDM+ categories. *$p \leq 0.05$, ***$p \leq 0.0001$.

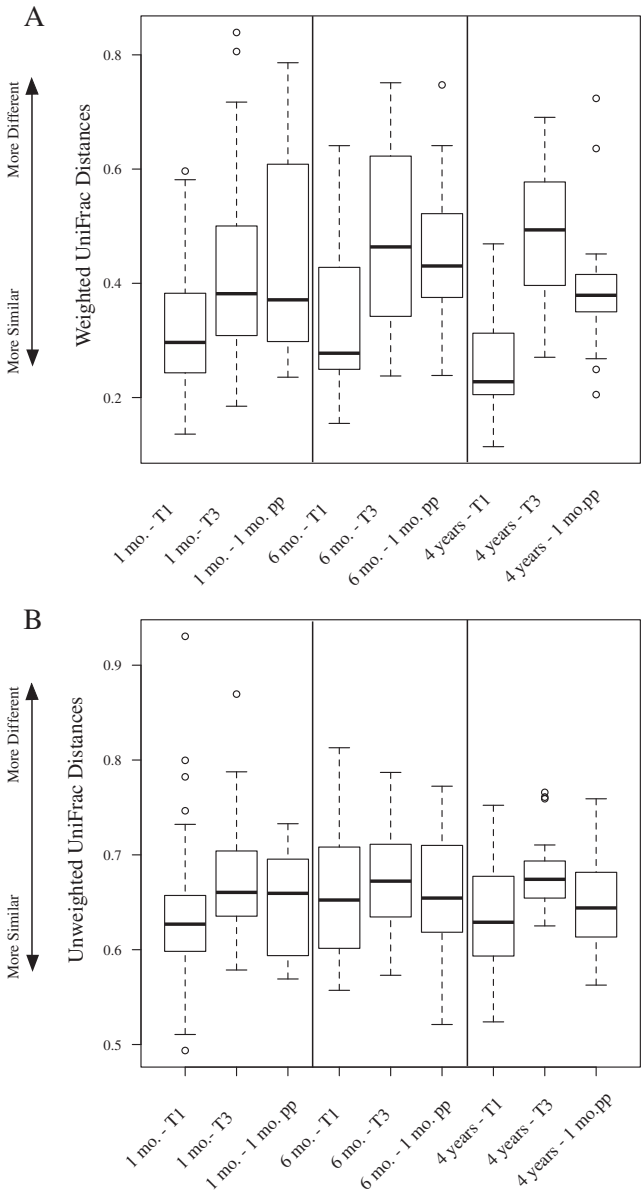

Figure S4. β-Diversity for Related Mother-Child Pairs, Related to Figure 4

Box plots for (A) weighted UniFrac and (B) unweighted UniFrac distances for mother-child pairs at different sampling times (mothers: T1, T3, post-partum; children: 1 month, 6 months, 4 years). For both plots the first 3 box plots on the left show distances between infants (1 mo) to their mothers sampled at T1, T3 and 1 month postpartum; the next set of 3 box plots shows similar distances for 6 months, and the last set of 3 shows the same analysis for the children sampled at 4 years of age.

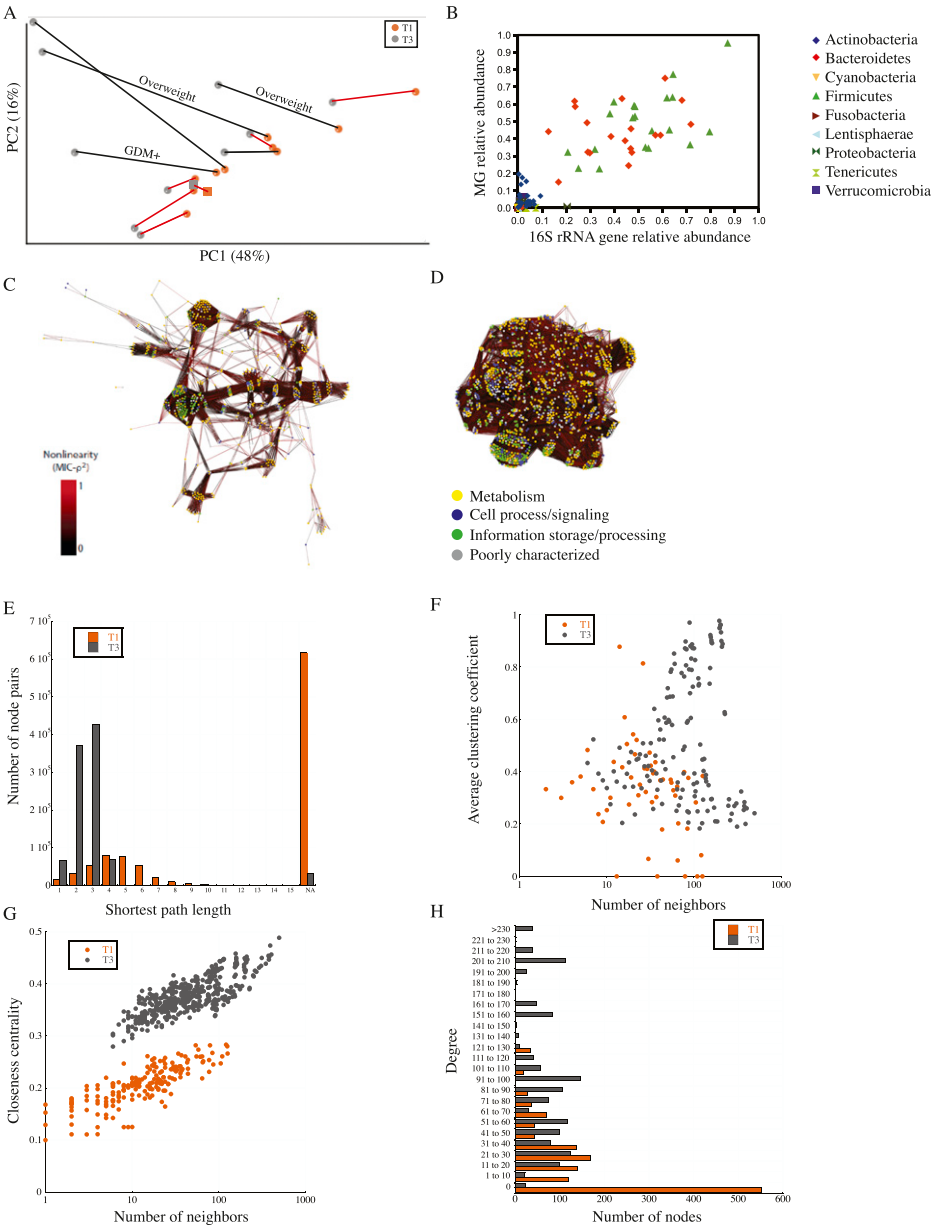

Figure S5. Shotgun Metagenomic Analysis of T1 and T3 Samples, Related to Figure 5

(A) PCoA of the weighted UniFrac distances for the mothers (circles) randomly selected for metagenomic analysis and the pooled inocula samples (squares). Samples were rarefied at 2,300 16S rRNA gene seqs/sample. See Figure S1 legend for details. Lines connect samples from the same individual, and the health state is indicated if different from normal. Samples connected with a red line were also used in the microbiota transplant experiment.

(B) A comparison of phylum level taxonomic relative abundance in 16S rRNA gene sequences versus phylogenetic data inferred from the metagenomes for the same samples. Metagenomic taxonomic assignments were based on MG-RAST lowest common ancestor taxonomic assignments to the M5NR database. Relative abundance in metagenomic data was calculated using the total abundance of reads assigned to the bacterial domain as denominator.

(C and D) Maximal information coefficient (MIC) based networks (for MIC = 1) for T1 and T3 generated from metagenomic COG relative abundance data. Networks were built separately from T1 (C; N = 10) and T3 (D; N = 10) samples, considering only the 1,392 COGs shared among all samples with a maximum abundance over 0.01% (552 unconnected COGs not shown in C; 24 unconnected COGs not shown in D). Nonlinearity scores of MIC relationships are indicated in the edge color key, and level-1 COG categories are indicated in the node color key.

(E–H) Parameters of MIC-based networks (built from the same shared 1,392 nodes) of T1 and T3 COG data: (E) Distribution of shortest path lengths between pairs of nodes. The rightmost data points, labeled "NA," were for node pairs with no connectedness (554 nodes in T1 and 24 in T3); (F) Average clustering coefficient (*C*) per node plotted as a function of the number of neighbors. Not shown are nodes with zero neighbors (*C* = 0; 552 nodes in T1; 24 nodes in T3) and nodes with only one neighbor (*C* = 1; 8 nodes in T1; 0 nodes in T3); (G) Closeness centrality of each node plotted as a function of the number of neighbors. Not shown are unconnected nodes (552 in T1 and 24 in T3) and nodes of small unconnected networks (2 nodes in T1). (H) Histogram of node degree values (in this case, degree = number of edges = number of neighbors). Node degrees ranged up to 124 for T1 and 495 for T3.

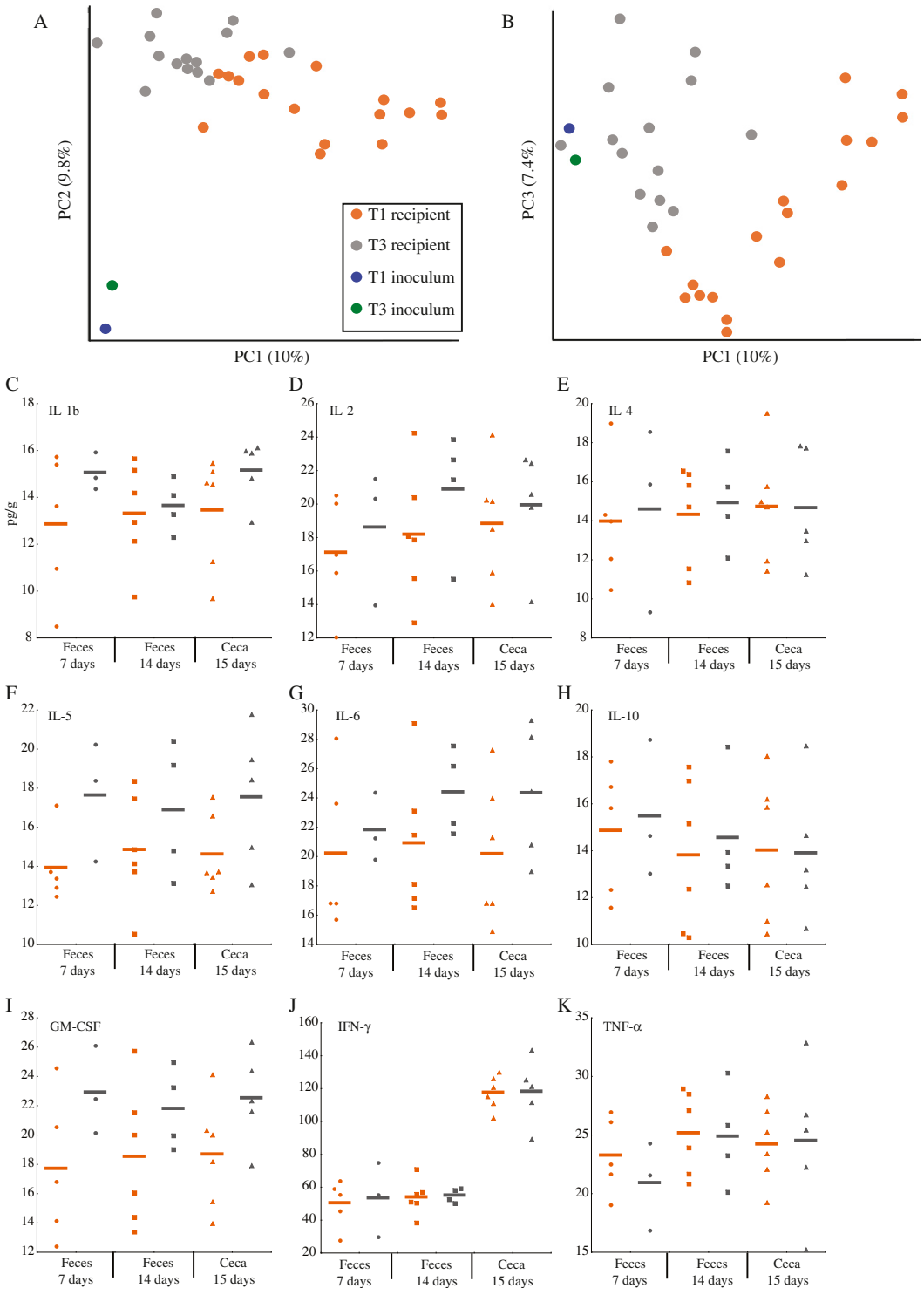

Figure S6. Transfer of Microbiota to GF Mice: Changes in Microbial Diversity and Inflammation, Related to Figure 6

(A and B) Diversity of gut microbiotas of GF mice 2 weeks after transfer of T1 and T3 inocula. PCoA of the unweighted UniFrac distances derived from the fecal (collected at 1 and 2 weeks) and cecal microbiotas (collected at 2 weeks) together with the pooled inocula samples. The percent variation explained by the PC's is indicated in parentheses on the axes.

(C–K) Mouse cytokine levels assessed in stool and cecal samples. Nine inflammation markers (IL-1β, 2, 4, 5, 6, 10, GM-CSF, IFN-γ and TNF-α) were measured in fecal samples after 7 and 14 days and in the cecal samples after 15 days of mice receiving T1 and T3 microbiotas. The units (pg/g) are indicated on the *y* axis of (C), and the same units apply to (D)–(K).